Archive for Rational Mechanics and Analysis manuscript No.
(will be inserted by the editor)

Non-laminate Microstructures in Monoclinic-I Martensite

Isaac Vikram Chenchiah · Anja Schlömerkemper

arXiv:1201.6679v2 [math.AP] 19 Jun 2012

Abstract We study the symmetrised rank-one convex hull of monoclinic-I martensite (a twelve-variant material) in the context of geometrically-linear elasticity. We construct sets of T_3s, which are (non-trivial) symmetrised rank-one convex hulls of three-tuples of pairwise incompatible strains. Moreover we construct a five-dimensional continuum of T_3s and show that its intersection with the boundary of the symmetrised rank-one convex hull is four-dimensional. We also show that there is another kind of monoclinic-I martensite with qualitatively different semi-convex hulls which, so far as we know, has not been experimentally observed.

Our strategy is to combine understanding of the algebraic structure of symmetrised rank-one convex cones with knowledge of the faceting structure of the convex polytope formed by the strains.

1 Introduction

Shape-memory alloys are materials that undergo a diffusionless solid-to-solid phase transformation due to change of temperature. They are capable of large macroscopic deformations and recover their original shape upon heating. While such materials usually form a cubic lattice (austenite) above a critical temperature they develop microstructures at lower temperatures (martensite). In this article we are interested in the cubic-to-monoclinic-I phase transformation, which occurs, eg., in NiTi, which is industrially one of the most important shape-memory alloys. In this case, there are twelve transformation strains, see Section 5 for details.

Isaac Vikram Chenchiah
School of Mathematics, University of Bristol, University Walk, Bristol BS8 1TW, UK. E-mail: Isaac.Chenchiah@bristol.ac.uk

Anja Schlömerkemper
Chair of Mathematics in the Sciences, Institute for Mathematics, University of Würzburg, Emil-Fischer-Str. 40, 97074 Würzburg, Germany. E-mail: Anja.Schloemerkemper@mathematik.uni-wuerzburg.de

Of interest is the set of all strains that can be recovered upon heating. In the variational approach to martensite [BJ87] this set is modelled by the quasiconvex hull (Definition 2.8) of the transformation strains. Unfortunately the quasiconvex hull of a set is difficult to calculate.

Bhattacharya and Kohn [BK97] consider various phase transformations (cubic to tetragonal, cubic to trigonal, cubic to orthorhombic and cubic to monoclinic) in the context of geometrically-linear elasticity and observe that except for cubic-to-monoclinic martensite the symmetrised quasiconvex hull coincides with the convex hull. For cubic-to-monoclinic martensite they show that the symmetrised quasiconvex hull is strictly smaller than the convex hull and present an inner bound for it.

We aim to find a better approximation of the symmetrised quasiconvex hull, again in the context of geometrically-linear elasticity. To this end, we are interested in the symmetrised lamination convex hull and the symmetrised rank-one convex hull of the transformation strains; these give inner bounds on the symmetrised quasiconvex hull, see Section 2.3.

Our analysis shows that there are points in the symmetrised rank-one convex hull of monoclinic-I martensite which are attained by *non-laminate* microstructures. This suggests (see below) that the symmetrised rank-one convex hull is strictly larger than the lamination convex hull of the twelve transformation strains. Since the symmetrised rank-one convex hull is a subset of the symmetrised quasiconvex hull (Remark 2.9), the strains attained by these non-laminate microstructures belong to the set of recoverable strains.

Next we give more details on the strategy we use, our results and the organisation of the paper. Finally we will fix some notation.

Strategy. Our strategy is to exploit firstly, the algebraic structure of symmetrised rank-one convex cones, secondly, the faceting structure of the convex hull of a finite set, and thirdly, the interaction between the two.

That rank-one convex cones are varieties has been exploited to develop algorithms to calculate semi-convex hulls [Kre03, KZC04]. The relevance of convex polytopes to semi-convex hulls (compare Lemma 2.10 with Theorem 2.11) has been noticed in [Zha06, TZ08] but has not, to our knowledge, been exploited to determine semi-convex hulls. This paper represents a first attempt in this direction.

The central idea is the following: Given a finite set whose symmetrised rank-one convex hull we wish to compute we proceed as follows. First we compute the symmetrised rank-one convex hulls of all its one-dimensional facets, i.e., edges in the language of convex polytopes; this is trivial, cf. (2.2) below. We use this, together with knowledge of the structure of symmetrised rank-one convex cones on two-dimensional affine subspaces (Section 3), to determine the symmetrised rank-one convex hulls of all its two-dimensional facets. We then repeat this for higher dimensions.

When the finite set we are interested in is the set of transformation strains of a material capable of a phase transformation from austenite to martensite, the set lies in the five-dimensional affine plane of strains with constant trace

and thus the process above terminates when the symmetrised rank-one convex hull of the five-dimensional facet of the set (which is the convex hull of the set) is computed.

In this bootstrapping strategy the steps become progressively more difficult as the dimension increases. Indeed while we can completely implement the two-dimensional step (Section 3 and [CSc]) and have partial results for the three-dimensional step [CSb] we have a reason to believe that the steps for dimension four and five are considerably more difficult than that for steps two and three: unlike in lower dimensions, the symmetrised rank-one convex cone in the higher dimensions is an algebraic surface of a polynomial which is necessarily irreducible [CSc].

Results. We have three main results:

First we show that there are two kinds of monoclinic-I martensites which differ qualitatively with regard to the polytope-structure of their convex hulls. It follows that their semi-convex hulls are qualitatively different as well. Curiously all known monoclinic-I martensites belong to one of these kinds, which we name monoclinic-Ia (the other being monoclinic-Ib).

The question as to whether T_3s (which are non-trivial symmetrised rank-one convex hulls of 3-tuples of pairwise incompatible strains, which are attained by non-laminate microstructures, see Section 4) can be formed from the twelve variants of Monoclinic-II martensite is raised in [BFJK94, p863]. There it is shown that this is possible when a certain lattice parameter is sufficiently small. Here we prove a stronger result: In Section 4 we present a simple test for T_3s (Lemma 4.3) that shows that in fact T_3s can form for all (non-zero) values of the lattice parameter, and that the same is true for Monoclinic-I martensite as well. This is our second main result.

Our third result is a consequence of this: We show that for Monoclinic-Ia martensite, the symmetrised rank-one convex hull of the twelve transformation strains contains a five-dimensional continuum of points which are attained by non-laminate microstructures. Moreover the intersection of this continuum with the boundary of the convex hull is four-dimensional. This suggests that the symmetrised rank-one convex hull of the transformation strains is strictly larger than the symmetrised lamination convex hull. This would then imply that the symmetrised quasiconvex envelope of the energy density of this material is different from the symmetrised lamination convex envelope. It is well known that lamination convex envelopes can differ from rank-one convex envelopes, cf. [Dac07, Sect. 4], and (in dimensions larger than two) that rank-one convex envelopes can differ from quasiconvex envelopes [Sve92]. However, in the context of materials science, all quasiconvex and rank-one convex envelopes that have been evaluated so far have in fact coincided with lamination convex envelopes; Monoclinic-Ia martensite is the first *material* for which we now have a strong indication that they differ.

Organisation of the paper. In Section 2 we refresh the reader's memory of some basic facts and results about strain compatibility, convex sets (in particular, convex polytopes) and semi-convex functions and sets.

In Section 3 we study the structure of symmetrised rank-one convex cones on two-dimensional affine subspaces of $\mathcal{S}_c^{3\times 3}$ (Lemma 3.1), see below for notation. The results presented here enable the computation of the symmetrised rank-one convex hull of any finite set in two-dimensional affine subspaces of $\mathcal{S}_c^{3\times 3}$ and the characterisation of those compact sets in these spaces that possess non-trivial symmetrised rank-one convex hulls; we present some results in Section 4 but postpone a more extensive discussion to [CSc]. We extend these results to higher dimensions in [CSb] but Lemma 4.10 and Section 7 provide a glimpse of the utility of the results in Section 4 even in higher dimensions.

We then turn from abstract results to the specific class of materials of interest to us, monoclinic-I martensite. After some preliminary observations in Section 5 on the compatibility and symmetry relations between the twelve transformation strains of materials in this class we determine, in Section 6, the facets of the convex hull of the twelve transformation strains of monoclinic-I martensite (Observations 6.6, 6.8 and 6.7). This leads to the discovery that there are in fact two kinds of monoclinic-I martensitic materials.

With this foundation behind us, in Section 7 we investigate the (theoretical) possibility of non-laminate zero-energy microstructures occurring in these materials. We construct an open set in the symmetrised rank-one convex hull of the transformation strains for which T_3-microstructures are optimal (Construction 7.5). We then deduce that in monoclinic-Ia martensite this set intersects the boundary of the convex hull, and thus the boundary of the symmetrised rank-one convex hull.

(In Sections 6 and 7 we use Mathematica to simplify computations but these computations are non-numerical. The Mathematica code that we have used together with explanatory notes can be found in the electronic supplementary material accompanying this article [CSa].)

We conclude with Section 8 with some questions raised by the preceding two sections. One of these is whether monoclinic-Ib martensite might have a larger set of recoverable strains (i.e., quasiconvex hull) than monoclinic-Ia martensite (modulo appropriate normalisation of the lattice parameters). This naturally also leads to the question as to whether a material that lies at the boundary of monoclinic-Ia and monoclinc-Ib martensite might demonstrate the best behaviour of all.

Notation. In the geometrically linear theory of elasticity, the strains (pointwise) belong to the space of real symmetric 3×3 matrices denoted by $\mathcal{S}^{3\times 3}$. We phrase some of our results for real symmetric $d \times d$ matrices and then use the symbol $\mathcal{S}^{d\times d}$. The space of real symmetric $d \times d$ matrices whose trace is an arbitrary (but fixed) constant c is denoted by $\mathcal{S}_c^{d\times d}$.

We introduce an inner product $\langle \cdot, \cdot \rangle$ on $\mathcal{S}^{d\times d}$ by $\mathcal{S}^{d\times d} \ni A, B \mapsto \langle A, B\rangle = \mathrm{Tr}(AB)$; the norm induced by this inner product is $\| \cdot \|$.

For $e_1, e_2 \in \mathcal{S}^{d\times d}$ we set

$$(e_1, e_2) := \{\lambda e_1 + (1-\lambda)e_2 \mid \lambda \in (0,1)\},$$
$$[e_1, e_2] := \{\lambda e_1 + (1-\lambda)e_2 \mid \lambda \in [0,1]\}.$$

By a *direction* in $\mathcal{S}^{d\times d}$ we mean a one-dimensional affine subspace of $\mathcal{S}^{d\times d}$. We denote the affine span of $S \subset \mathcal{S}^{d\times d}$ by $\operatorname{aff span}(S)$, the relative boundary of $S \subset \mathcal{S}^{d\times d}$ by $\operatorname{rel}\partial S$ and its relative interior by $\operatorname{rel int} S$.

2 Preliminaries

2.1 Strain compatibility

Definition 2.1 (Strain compatibility) Let $e_1, e_2 \in \mathcal{S}^{3\times 3}$ and $S_1, S_2 \subset \mathcal{S}^{3\times 3}$.

1. e_1 is compatible with e_2 (or e_1 and e_2 are compatible), $e_1 \mid\!\mid\!\mid e_2$, if there exist $a, b \in \mathbb{R}^3$ such that $e_1 - e_2 = \frac{1}{2}(a\otimes b + b \otimes a)$, where $\otimes$ denotes the dyadic product.
2. e_1 is compatible with 0 (or compatible for short) if $e_1 \mid\!\mid\!\mid 0$.
3. e_1 is incompatible with e_2 (or e_1 and e_2 are incompatible), $e_1 \not\mid\!\mid\!\mid e_2$, if e_1 and e_2 are not compatible.
4. e_1 is incompatible with 0 (or incompatible for short) if $e_1 \not\mid\!\mid\!\mid 0$.
5. S_1 is totally compatible with S_2 (or S_1 and S_2 are totally compatible), $S_1 \mid\!\mid\!\mid S_2$, if for all $e_1 \in S_1$ and for all $e_2 \in S_2$, $e_1 \mid\!\mid\!\mid e_2$.
6. S_1 is compatible if $S_1 \mid\!\mid\!\mid S_1$, i.e., if for all $e_1, e_2 \in S_1$, $e_1 \mid\!\mid\!\mid e_2$.
7. S_1 is totally incompatible with S_2 (or S_1 and S_2 are totally incompatible), $S_1 \not\mid\!\mid\!\mid S_2$, if for all $e_1 \in S_1$ and for all $e_2 \in S_2$, $e_1 \not\mid\!\mid\!\mid e_2$.

We observe that $[e_1, e_2]$ is compatible if and only if $e_1 \mid\!\mid\!\mid e_2$. An alternative term for compatibility is "symmetrised rank-one connectedness".

In the figures compatible lines are represented by solid lines and incompatible lines by dashed lines, cf. eg. Figure 4.1. The following lemma follows immediately from [Koh91, Lemma 4.1].

Lemma 2.2 (Compatibility in $\mathcal{S}^{3\times 3}_c$) *Let $e_1, e_2 \in \mathcal{S}^{3\times 3}_c$. Then $e_1 \mid\!\mid\!\mid e_2$ iff* $\det(e_1 - e_2) = 0$.

Definition 2.3 (Compatible cone) Let $S \subset \mathcal{S}^{3\times 3}_c$ and $x \in S$. The compatible cone in S at x is the set

$$\Lambda_{S,x} := \{y \in S \mid y \mid\!\mid\!\mid x\}.$$

When $0 \in S$ we set $\Lambda_S := \Lambda_{S,0}$.

Note that the compatible cone $\Lambda_{S,x}$ is an affine cone with vertex x in the linear algebraic sense, i.e., it is closed under multiplication by positive reals. However, the compatible cone is not geometrically a cone.

2.2 Convex sets

We recall some elementary definitions and results from convex analysis. For more details see, eg. [Roc96].

Let E be a subset of a vector space. We denote the convex hull of E by $\mathcal{C}(E)$.

Definition 2.4 (Extreme subsets of convex sets) Let $S \subset \mathbb{R}^d$ be convex. Then $S' \subseteq S$ is an *extreme subset* of S if S' is convex and satisfies: If $x, y \in S$ and $\exists \lambda \in (0,1)$ such that $\lambda x + (1-\lambda)y \in S'$, then $x, y \in S'$.

Of special interest to us are *convex polytopes* which are convex hulls of finite sets. Definition 2.5 and Remark 2.6 suffice for us. For an introduction to convex polytopes we refer the reader to, eg. [Bar03, Brø82, Ewa96, Grü03, Gru07, Zie94].

Definition 2.5 (Vertices, edges and facets of convex polytopes) The vertices of a convex polytope are its extreme points, its edges are its one-dimensional extreme subsets and its facets are its extreme subsets with co-dimension one.

Let E be a finite set. We denote the set of n-dimensional extreme subsets of $\mathcal{C}(E)$ by $\mathcal{F}_n(E)$. Thus the set of vertices of $\mathcal{C}(E)$ is $\mathcal{F}_0(E)$, the set of its edges is $\mathcal{F}_1(E)$, and the set of facets is $\mathcal{F}_{\dim(\mathcal{C}(E))-1}(E)$ and $\mathcal{F}_{\dim \mathcal{C}(E)}(E) = \{\mathcal{C}(E)\}$.

Remark 2.6 For $S \in \mathcal{F}_n(E)$, $n = 1, \ldots, \dim(\mathcal{C}(E))$, the relative boundary $\operatorname{rel} \partial S$ is a union of elements of $\mathcal{F}_{n-1}(E)$.

2.3 Semi-convex functions and sets

Next we recall some elementary definitions and results about semi-convex functions and sets. For more details see, eg. [Mül99, Dac07]. Since we work in the context of $S^{d\times d}$ (as opposed to $R^{d\times d}$) we have appended the qualifier "symmetrised" to the various notions of semi-convexity. The qualifier "symmetric" is also used in the literature.

The term "symmetrised rank-one convex" (Defintion 2.8 below) might be misleading in that the matrices involved need not be of rank one but rather are the symmetric parts of rank-one matrices. An alternative name could be "wave-cone convex", because the symmetric tensor products form the wave cone of a second-order linear differential operator whose kernel are the symmetrised gradients [Tar79, Mur07].

Definition 2.7 (Semi-convex functions)

1. $f\colon S^{d\times d} \to \mathbb{R}$ is symmetrised rank-one convex if for all $\lambda \in [0,1]$

$$f(\lambda e_1 + (1-\lambda)e_2) \leqslant \lambda f(e_1) + (1-\lambda) f(e_2) \quad \forall e_1, e_2 \in S^{d\times d} \text{ with } e_1 \,|||\, e_2.$$

2. A locally-bounded Borel function $f\colon S^{d\times d}\to\mathbb{R}$ is symmetrised quasiconvex if for an open and bounded set $U\subset\mathbb{R}^d$ with $|\partial U|=0$ one has

$$f(e)\leqslant\frac{1}{|U|}\int_U f(e+D_s\varphi)\,dx\quad\forall\varphi\in W_0^{1,\infty}(U,\mathbb{R}^d),$$

whenever the integral on the right hand side exists, where $D_s\varphi$ is the symmetrised gradient of φ.

Definition 2.8 (Semi-convex sets) Let E be a compact set in $S^{d\times d}$.

1. The symmetrised quasiconvex hull of E is defined as

$$\mathcal{Q}(E):=\{e\in S^{d\times d}\,|\,f(e)\leqslant\sup_{e'\in E}f(e')\quad\forall f\colon S^{d\times d}\to\mathbb{R}\text{ quasiconvex}\}.$$

2. The symmetrised rank-one convex hull of E is defined as

$$\mathcal{R}(E):=\{e\in S^{d\times d}\,|\,f(e)\leqslant\sup_{e'\in E}f(e')\quad\forall f\colon S^{d\times d}\to\mathbb{R}\text{ symmetrised rank-one convex}\}.$$

3. The symmetrised lamination convex hull of E, $\mathcal{L}(E)$, is the smallest set $\widetilde{E}\supseteq E$ such that $e_1,e_2\in\widetilde{E}$ and $e_1\,|||\,e_2$ implies that $[e_1,e_2]\subset\widetilde{E}$.

We note that symmetrised lamination convex hulls can be constructed as follows: For $n\in\mathbb{N}_0$, let

$$\begin{aligned}\mathcal{L}_0(E)&:=E,\\ \mathcal{L}_{n+1}(E)&:=\{e\mid\exists e_1,e_2\in\mathcal{L}_n(E),\ e_1\,|||\,e_2,\ e\in[e_1,e_2]\}.\end{aligned}$$

Then,

$$\mathcal{L}(E)=\bigcup_{n\in\mathbb{N}_0}\mathcal{L}_n(E).$$

Symmetrised rank-one convex hulls also have an alternate characterisation (cf. eg. [Kre03, Lemma 2.5]):

$$\mathcal{R}(E):=\{e\in S^{d\times d}\,|\,f(e)=0\forall f\colon S^{d\times d}\to[0,\infty)\text{ symmetrised rank-one convex with }f(E)=\{0\}\}.\quad(2.1)$$

We shall repeatedly use Remark 2.9 and Lemma 2.10 without explicitly citing them:

Remark 2.9 $\mathcal{L}(E)\subseteq\mathcal{R}(E)\subseteq\mathcal{Q}(E)\subseteq\mathcal{C}(E)$.

Lemma 2.10 ([Bha93, Section 3.4.1, p. 231]) *Let $E\subset\mathcal{S}^{d\times d}$ be finite and compatible. Then $\mathcal{L}(E)=\mathcal{C}(E)$.*

In particular,

$$\forall x, y \in \mathcal{S}^{3\times 3}_c, \quad \mathcal{R}(\{x,y\}) = \begin{cases} [x,y] & \text{if } x \,|||\, y, \\ \{x,y\} & \text{else.} \end{cases} \tag{2.2}$$

Lemma 2.10 however is too weak for our purposes; we present a sharp version [Zha06, p.38][TZ08, p.1266]:

Theorem 2.11 *Let $E \subset \mathcal{S}^{d\times d}$ be finite. Then $\mathcal{L}(E) = \mathcal{C}(E)$ if and only if every edge of $\mathcal{C}(E)$ is compatible, i.e., if and only if*

$$\forall e_1, e_2 \in E, \qquad e_1 \not\| e_2 \implies [e_1, e_2] \notin \mathcal{F}_1(E).$$

Proof Necessity. Let $[e_1, e_2] \in \mathcal{F}_1(E)$ with $e_1 \not\| e_2$. We show that $(e_1, e_2) \not\subset \mathcal{L}(E)$:

Let $e \in [e_1, e_2]$ and $e \in \mathcal{L}(E)$. Then $\exists n \in \mathbb{N}$ finite, $f_1, f_2 \in \mathcal{L}_n(E)$ such that $e \in [f_1, f_2]$. However by extremality of $[e_1, e_2]$, $f_1, f_2 \in [e_1, e_2]$. Applying the same argument to f_1 and f_2 we conclude that in fact $e \in \mathcal{L}(\{e_1, e_2\})$ but from (2.2), $\mathcal{L}(\{e_1, e_2\}) = \{e_1, e_2\}$. Thus $e \in [e_1, e_2]$ and $e \in \mathcal{L}(E) \implies e \in \{e_1, e_2\}$.

Sufficiency. Let every edge of $\mathcal{C}(E)$ be compatible. We show by induction that

$$S \in \mathcal{F}_n(E) \implies S \subseteq \mathcal{L}_n(E). \tag{P_n}$$

for $n = 0, 1, \ldots, \dim(\mathcal{C}(E))$. Since $(P_{\dim(\mathcal{C}(E))})$ is the statement that $\mathcal{C}(E) \subseteq \mathcal{L}(E)$, the result follows from Remark 2.9.

(P_0) is trivially true since $e \in \mathcal{F}_0$ implies $e \in E$ and thus $e \in \mathcal{L}_0(E)$; (P_1) is true since every edge of $\mathcal{C}(E)$ is compatible by assumption. Now let (P_n) be true for some fixed $n = 1, \ldots, \dim(\mathcal{C}(E)) - 1$. We show that (P_{n+1}) is true:

Let $S \in \mathcal{F}_{n+1}(E)$ and $e \in S$. If $e \in \operatorname{rel}\partial S$, then e is contained in an element of $\mathcal{F}_n(E)$ (Remark 2.6) and thus, by the inductive hypothesis, $e \in \mathcal{L}_n(E) \subset \mathcal{L}_{n+1}(E)$. We consider the case $e \in \operatorname{rel}\operatorname{int} S$:

Pick $v \in \mathcal{F}_1(E) \cap \operatorname{rel}\partial S$. We view v as a vector in $\mathcal{S}^{d\times d}$. Since S is bounded, the inclusion

$$e + \lambda v \in \operatorname{rel}\partial S, \quad \lambda \in \mathbb{R},$$

has two solutions $\lambda_- < 0$ and $\lambda_+ > 0$. Note that $(e + \lambda_+ v) - (e + \lambda_- v)$ is parallel to v, which is compatible (by assumption). Thus $e + \lambda_\pm v \in \mathcal{L}_n(E)$ (by (P_n)), $e + \lambda_- v \,|||\, e + \lambda_+ v$ and

$$e = \frac{\lambda_+}{\lambda_+ - \lambda_-}(e + \lambda_- v) + \frac{-\lambda_-}{\lambda_+ - \lambda_-}(e + \lambda_+ v).$$

It follows that $e \in \mathcal{L}_{n+1}(E)$ and thus $S \subseteq \mathcal{L}_{n+1}(E)$.

3 The compatible cone in two-dimensional affine subspaces of $\mathcal{S}_c^{3\times 3}$

Our first task is to characterise, both geometrically (Lemma 3.1) and algebraically (Remark 3.7), the symmetrised rank-one convex cone in two-dimensional affine subspaces of $\mathcal{S}_c^{3\times 3}$.

Lemma 3.1 *Let S be a two-dimensional subspace of $\mathcal{S}_c^{3\times 3}$. Then either*

1. *S contains precisely one, two or three compatible directions, or*
2. *S is compatible.*

Proof Let $\{e_1, e_2\}$ be a basis for S. By Lemma 2.2, an arbitrary non-zero element of S, $xe_1 + ye_2$, $(x, y) \neq 0$, is compatible iff

$$\det(xe_1 + ye_2) = 0.$$

This is equivalent to

$$x^3 \det(e_1) + x^2 y \langle \operatorname{cof}(e_1), e_2 \rangle + xy^2 \langle e_1, \operatorname{cof}(e_2) \rangle + y^3 \det(e_2) = 0, \tag{3.1}$$

where $\operatorname{cof}(e)$ is the cofactor of e:

$$\operatorname{cof} \begin{pmatrix} e_{11} & e_{12} & e_{13} \\ e_{21} & e_{22} & e_{23} \\ e_{31} & e_{32} & e_{33} \end{pmatrix} = \begin{pmatrix} e_{22}e_{33} - e_{32}e_{23} & -(e_{21}e_{33} - e_{31}e_{23}) & e_{21}e_{32} - e_{31}e_{22} \\ -(e_{12}e_{33} - e_{32}e_{13}) & e_{11}e_{33} - e_{31}e_{13} & -(e_{11}e_{32} - e_{31}e_{12}) \\ e_{12}e_{23} - e_{22}e_{13} & -(e_{11}e_{23} - e_{21}e_{13}) & e_{11}e_{22} - e_{21}e_{12} \end{pmatrix}^T.$$

If the polynomial in (3.1) is the zero-polynomial (i.e., $\det(e_1) = 0, \langle \operatorname{cof}(e_1), e_2 \rangle = 0$ etc.) then S is compatible. Otherwise:

If either $\det(e_1) = 0$ or $\det(e_2) = 0$ then (3.1) has one or two solutions $(x, y) \neq 0$ and thus S contains one or two compatible directions. Assume on the contrary that both $\det(e_1)$ and $\det(e_2) \neq 0$. Since $(x, y) \neq 0$, dividing (3.1) by either x^3 or y^3 we obtain a polynomial (in either $\frac{x}{y}$ or $\frac{y}{x}$) which, being cubic, has one, two or three distinct real roots. Thus S contains one, two or three compatible directions.

Corollary 3.2 *Let S be a subspace of $\mathcal{S}_c^{3\times 3}$ with $\dim(S) > 1$. Then S contains at least one compatible direction.*

The following examples show that each of the possibilities referred to in Lemma 3.1 can occur:

Example 3.3 (One compatible direction)
The determinant of these matrices is proportional to $x(x^2 + y^2)$ so the compatible direction is $x = 0$:

$$\left\{ \begin{pmatrix} x & 0 & 0 \\ 0 & x & y \\ 0 & y & -2x \end{pmatrix} \middle| \, x, y \in \mathbb{R} \right\}.$$

The determinant of these matrices is proportional to x^3 so the compatible direction is $x = 0$:

$$\left\{ \begin{pmatrix} y & x & x \\ x & -y & x \\ x & x & 0 \end{pmatrix} \middle| \, x, y \in \mathbb{R} \right\}.$$

Example 3.4 (Two compatible directions) The determinant of these matrices is proportional to xy^2 so the two compatible directions are $x = 0$ and $y = 0$:

$$\left\{ \begin{pmatrix} x & 0 & 0 \\ 0 & -x & y \\ 0 & y & 0 \end{pmatrix} \middle| \, x, y \in \mathbb{R} \right\}.$$

Example 3.5 (Three compatible directions)

The determinant of these matrices is proportional to $xy(x+y)$ so the three compatible directions are $x = 0$, $y = 0$ and $x = -y$:

$$\left\{ \begin{pmatrix} x & 0 & 0 \\ 0 & y & 0 \\ 0 & 0 & -x-y \end{pmatrix} \middle| \, x, y \in \mathbb{R} \right\}.$$

The determinant of these matrices is proportional to $x(x^2 - y^2)$ so the three compatible directions are $x = 0$, $x = y$ and $x = -y$:

$$\left\{ \begin{pmatrix} -2x & 0 & 0 \\ 0 & x & y \\ 0 & y & x \end{pmatrix} \middle| \, x, y \in \mathbb{R} \right\}.$$

Example 3.6 (Compatible (two-dimensional) plane)

$$\left\{ \begin{pmatrix} 0 & 0 & 0 \\ 0 & x & y \\ 0 & y & -x \end{pmatrix} \middle| \, x, y \in \mathbb{R} \right\}, \quad \left\{ \begin{pmatrix} 0 & x & y \\ x & 0 & 0 \\ y & 0 & 0 \end{pmatrix} \middle| \, x, y \in \mathbb{R} \right\}.$$

We note that Lemma 3.1 follows also from the following characterisation of real homogeneous cubic polynomials in two variables:

Remark 3.7 A homogeneous cubic polynomial on $\mathbb{R}^2$ can, by an appropriate choice of basis, be written in precisely one of the five following forms cf. eg. [Gur64, Sec.23, p.263-6],[Wei88] or [Olv99, p.28]:

1. $x(x^2 + y^2)$,
2. x^3,
3. xy^2,
4. $xy(x + y)$ or, equivalently, $x(x^2 - y^2)$,
5. 0.

The examples above illustrate these possibilities.

Lemma 3.1 shows that from the perspective of symmetrised rank-one convexity there are four kinds of two-dimensional affine subspaces of $\mathcal{S}_c^{3\times 3}$, namely those for which the compatible cone is

1. a line,
2. the union of two (distinct) lines,
3. the union of three (distinct) lines, and
4. the subspace itself.

The next step is to investigate compatible hulls in these subspaces. Cases (1) and (4) are the simplest: In Case (1) compatible hulls are obtained by convexifying in the compatible direction, in Case (4) compatible hulls are identical to convex hulls.

Cases (2) and (3) are reminiscent of separate convexity in $\mathbb{R}^2$ [Tar93, Kre03]: Symmetrised rank-one convexity is *geometrically* identical to separate convexity in $\mathbb{R}^2$ in Case (2), and is similar to separate convexity in $\mathbb{R}^2$ in Case (3). As an aside, the inclusion-minimal configurations [SJ05] in these situations are either $T_3 s$ or $T_4 s$ as might be expected. Only T_3s are relevant to our immediate purposes so we discuss them in Section 4 and leave the rest for [CSc].

4 T_3s

$T3$s occur when there are precisely three directions in the compatible cone. Our definition is equivalent/identical to earlier definitions in the literature such as [BFJK94][p. 855, (3.9) on p. 862 and Fig. 3.1b on p. 856].

Definition 4.1 **(T_3)** Three points $e_1, e_2, e_3 \in \mathcal{S}_c^{3\times 3}$ form a T_3 if

1. They are pairwise incompatible, and
2. There exist $e_{1,1} \in (e_2, e_3), e_{2,2} \in (e_3, e_1), e_{3,3} \in (e_1, e_2)$ such that $e_{i,i} \,|||\, e_i$, $i = 1, 2, 3$.

A schematic representation of a T_3 is shown in Figure 4.1.

Remark 4.2 Note that $\operatorname{span}\{e_1 - e_{1,1}\}$, $\operatorname{span}\{e_2 - e_{2,2}\}$ and $\operatorname{span}\{e_3 - e_{3,3}\}$ are distinct compatible directions. By Lemma 3.1 there are no others. It follows that $e_{1,1}$, $e_{2,2}$ and $e_{3,3}$ are unique.

Next we show that it is easy to check whether three points form a T_3:

Lemma 4.3 *Three points $e_1, e_2, e_3 \in \mathcal{S}_0^{3\times 3}$ form a T_3 if and only if*

$$\operatorname{sign}\det(e_1 - e_2) = \operatorname{sign}\det(e_2 - e_3) = \operatorname{sign}\det(e_3 - e_1) \neq 0. \tag{4.1}$$

Proof Let $e_1, e_2, e_3 \in \mathcal{S}_0^{3\times 3}$ satisfy (4.1). From Lemma 2.2 it follows immediately that Definition 4.1(1) is satisfied. Consider the polynomial $[0, 1] \ni \lambda \mapsto \det((\lambda e_1 + (1-\lambda)e_2) - e_3)$. By assumption, this polynomial has opposite signs at 0 and 1. In conjunction with Lemma 2.2 this implies:

$$\exists \lambda_{12} \in (0, 1), \quad e_{3,3} := (\lambda_{12} e_1 + (1 - \lambda_{12}) e_2) \,|||\, e_3. \tag{4.2a}$$

Similarly,

$$\exists \lambda_{23} \in (0, 1), \quad e_{1,1} := (\lambda_{23} e_2 + (1 - \lambda_{23}) e_3) \,|||\, e_1, \tag{4.2b}$$

$$\exists \lambda_{31} \in (0, 1), \quad e_{2,2} := (\lambda_{31} e_3 + (1 - \lambda_{31}) e_1) \,|||\, e_2. \tag{4.2c}$$

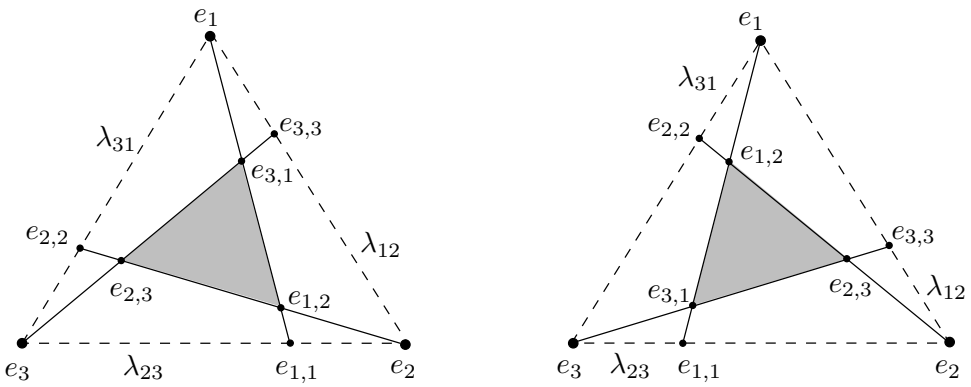


Fig. 4.1: Schematic representations of points forming T_3s.

This shows that Definition 4.1(2) is satisfied. Thus $\{e_1, e_2, e_3\}$ forms a T_3.

Conversely, assume that $\{e_1, e_2, e_3\} \subset \mathcal{S}_0^{3\times 3}$ form a T_3. Then, from Definition 4.1(1), $\operatorname{sign}\det(e_1 - e_2), \operatorname{sign}\det(e_2 - e_3), \operatorname{sign}\det(e_3 - e_1) \neq 0$. Suppose it is *not* the case that $\operatorname{sign}\det(e_1 - e_2) = \operatorname{sign}\det(e_2 - e_3) = \operatorname{sign}\det(e_3 - e_1)$. Then, relabelling the points if necessary, we have

$$\det(e_1 - e_3), \det(e_2 - e_3) > 0. \tag{4.3}$$

Now consider the cubic polynomial $\mathbb{R} \ni \lambda \mapsto \det((\lambda e_1 + (1-\lambda)e_2) - e_3)$. By assumption there are three compatible directions passing through e_3, which are parallel to $[e_1, e_{1,1}]$, $[e_2, e_{2,2}]$ and $[e_3, e_{3,3}]$; see Figure 4.1. Thus the cubic polynomical has three distinct real roots, one in each of $(-\infty, 0)$, $(0, 1)$ and $(1, \infty)$. Thus each root is simple; it follows that the polynomial changes sign around each root.

On the other hand from (4.3) the polynomial is positive at 0 and 1. It follows that it has one further root in $(0, 1)$, which is a contradiction. We conclude that $\operatorname{sign}\det(e_1 - e_2) = \operatorname{sign}\det(e_2 - e_3) = \operatorname{sign}\det(e_3 - e_1)$.

Definition 4.4 (Vertices of a T_3) Let $e_1, e_2, e_3 \in \mathcal{S}_c^{3\times 3}$ form a T_3 as in Definition 4.1. Then e_1, e_2, e_3 are referred to as the vertices of this T_3.

When $e_1, e_2, e_3 \in \mathcal{S}_c^{3\times 3}$ form a T_3 then their symmetrised rank-one convex hull $\mathcal{R}(\{e_1, e_2, e_3\})$ is (also) called a T_3. The context will make clear whether "T_3" refers to the set of three strains $\{e_1, e_2, e_3\}$ or to their symmetrised rank-one convex hull $\mathcal{R}(\{e_1, e_2, e_3\})$.

It is known (cf., e.g., [BFJK94, §3]) that

$$\mathcal{R}(\{e_1, e_2, e_3\}) \supseteq [e_1, e_{1,2}] \cup [e_2, e_{2,3}] \cup [e_3, e_{3,1}] \cup \mathcal{C}(\{e_{1,2}, e_{2,3}, e_{3,1}\}), \tag{4.4}$$

where $e_{1,2}$, $e_{2,3}$, $e_{3,1}$ are the nodes of the T_3 (Definition 4.5 below), see Figure 4.2. However for the convenience of the reader we provide a proof of this in Proposition 4.9 below.

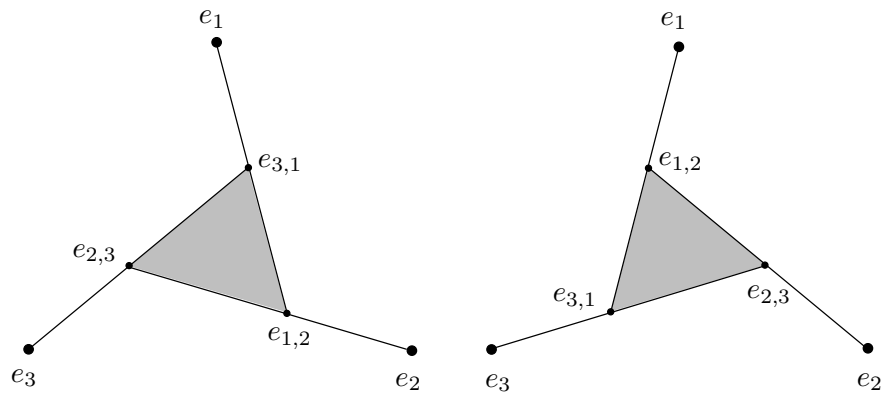


Fig. 4.2: Schematic representations of T_3s, i.e. the rank-one convex hull of three strains forming a T_3.

Definition 4.5 (Nodes of a T_3) Let $e_1, e_2, e_3 \in \mathcal{S}_c^{3\times 3}$ form a T_3. Let $e_{1,1}$, $e_{2,2}$, $e_{3,3}$ be as defined in (4.2a)–(4.2c). We define the nodes of the T_3 to be the three points

$$e_{i,j} := [e_i, e_{i,i}] \cap [e_j, e_{j,j}], \quad i \neq j,\ i,j = 1,2,3$$

(see Figure 4.1).

From Definition 4.1(2) the nodes of a T_3 are pair-wise compatible and $e_{i,j}$ is compatible with e_i and e_j.

Later we will encounter symmetric T_3s and similar T_3s as defined below:

Definition 4.6 (Symmetric T_3s) Let $e_1, e_2, e_3 \in \mathcal{S}_c^{3\times 3}$ form a T_3. Let λ_{12}, λ_{23}, λ_{31} be as defined in (4.2a)–(4.2c). Then the T_3 is symmetric if $\lambda_{12} = \lambda_{23} = \lambda_{31}$.

The following remark is elementary but we explicitly state it since it arises frequently in applications (cf. Section 7):

Remark 4.7 Let $R \in SO(3)$ such that R^3 is the identity. Let $e_1 \in \mathcal{S}_c^{3\times 3}$, $e_2 := R^T e_1 R$ and $e_3 := R^T e_2 R$. Then $\det(e_1 - e_2) = \det(e_2 - e_3) = \det(e_3 - e_1)$ and if this is non-zero then e_1, e_2, e_3 form a symmetric T_3.

Definition 4.8 (Similar T_3s) Let $e_1, e_2, e_3 \in \mathcal{S}_c^{3\times 3}$ and $e_1', e_2', e_3' \in \mathcal{S}_c^{3\times 3}$ form T_3s. Let λ_{ij}, λ_{ij}', $i \neq j$, $i,j = 1,2,3$ be defined as in (4.2).

1. We say that these T_3s are similar if, for some permutation $\sigma\colon \{1,2,3\} \to \{1,2,3\}$, $\lambda_{12}' = \lambda_{\sigma(1)\sigma(2)}$, $\lambda_{23}' = \lambda_{\sigma(2)\sigma(3)}$ and $\lambda_{31}' = \lambda_{\sigma(3)\sigma(1)}$.
2. Corresponding points in these T_3s are points with the same barycentric coordinates: For $\mu_1, \mu_2, \mu_3 \in [0,1]$, $\sum_{i=1}^3 \mu_i = 1$, $\mu_1 e_1 + \mu_2 e_2 + \mu_3 e_3$ and $\mu_1 e_{\sigma(1)}' + \mu_2 e_{\sigma(2)}' + \mu_3 e_{\sigma(3)}'$ are corresponding points where σ is the permutation in item (1) above.

We now prove (4.4):

Proposition 4.9 *Let $e_1, e_2, e_3 \in \mathcal{S}_c^{3\times 3}$ form a T_3. Then*

$$\mathcal{R}(\{e_1, e_2, e_3\}) \supseteq [e_1, e_{1,2}] \cup [e_2, e_{2,3}] \cup [e_3, e_{3,1}] \cup \mathcal{C}(\{e_{1,2}, e_{2,3}, e_{3,1}\}). \quad (4.4)$$

Proof We use the same strategy as [Kre03, Proposition 2.7]. Let $e_{1,2}$, $e_{2,3}$, $e_{3,1}$ be related to e_1, e_2, e_3 as in the left-hand side of Figures 4.1 and 4.2; the proof in the other case is similar.

Let f be non-negative, symmetrised rank-one convex and vanish on $\{e_1, e_2, e_3\}$. Since $e_1 \,|||\, e_{1,2}$, it follows from the convexity of f on $[e_1, e_{1,2}]$ that $f(e_{1,2}) \geqslant f(e_{3,1})$. Similarly, since $e_2 \,|||\, e_{2,3}$, it follows that $f(e_{2,3}) \geqslant f(e_{1,2})$. Finally from $e_3 \,|||\, e_{3,1}$ it follows that $f(e_{3,1}) \geqslant f(e_{2,3})$. In other words, $f(e_{2,3}) \geqslant f(e_{1,2}) \geqslant f(e_{3,1}) \geqslant f(e_{2,3})$. We conclude that $f(e_{2,3}) = f(e_{1,2}) = f(e_{3,1}) = f(e_{2,3})$. But since $f(e_1) = 0$, convexity of f on $[e_1, e_{1,2}]$ shows that in fact $f(e_{1,2}) = f(e_{2,3}) = f(e_{3,1}) = 0$. From (2.1) we conclude that

$$[e_1, e_{1,2}] \cup [e_2, e_{2,3}] \cup [e_3, e_{3,1}] \subset \mathcal{R}(\{e_1, e_2, e_3\}).$$

The last step is to notice that since $e_{1,2}$, $e_{2,3}$, $e_{3,1}$ are pair-wise compatible, from Lemma 2.10,

$$\mathcal{C}(\{e_{1,2}, e_{2,3}, e_{3,1}\}) \subset \mathcal{R}(\{e_1, e_2, e_3\}),$$

which completes the proof.

We end this section by giving an example of the utility of two-dimensional results in higher dimensions.

Lemma 4.10 (A three-dimensional continuum of T_3s) *Let $e_1, e_2, e_3 \in \mathcal{S}_c^{3\times 3}$ form a T_3. Let $e_0 \in \mathcal{S}_c^{3\times 3}$ such that $e_i \,|||\, e_0$ for $i = 1, 2, 3$. For $\lambda \in \mathbb{R}$ and $i = 1, 2, 3$ let*

$$e_i^\lambda := \lambda e_0 + (1 - \lambda) e_i.$$

Then $e_1^\lambda, e_2^\lambda, e_3^\lambda$ also form a T_3 and

$$\bigcup_{\lambda\in[0,1]} \mathcal{R}(\{e_1^\lambda, e_2^\lambda, e_3^\lambda\}) \subseteq \mathcal{R}(\{e_0, e_1, e_2, e_3\}) \quad (4.5)$$

which, when $e_0 \notin \operatorname{aff}\operatorname{span}\{e_1, e_2, e_3\}$, is a three-dimensional continuum of T_3s.

Proof Let $\lambda \in (0, 1)$ and $i = 1, 2, 3$. Since $e_0 ||| e_i$ it follows that $e_i^\lambda \in \mathcal{L}(\{e_0, e_1, e_2, e_3\})$. Since $\operatorname{sign}\det(e_i^\lambda - e_j^\lambda) = \operatorname{sign}\det(e_i - e_j)$, $i, j = 1, 2, 3$, it follows that $e_1^\lambda, e_2^\lambda, e_3^\lambda$ form a T_3. The result follows.

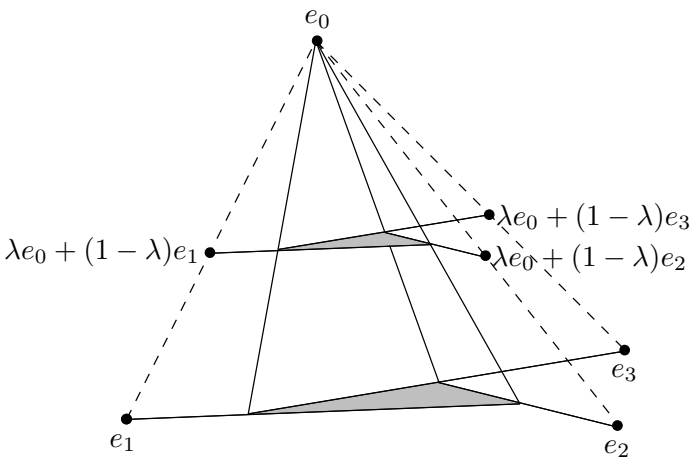


Fig. 4.3: The three-dimensional continuum of T_3s described in Lemma 4.10.

5 The transformation strains of Monoclinic-I martensite

In this and the next section we prepare to apply the results of the preceding sections to monoclinic-I martensite by exploring first the symmetry and the geometry of this material.

We denote the transformation strains of the twelve variants of cubic-to-monoclinic-I martensite, listed in Table 5.1, by

$$e^{(i)} \in \mathcal{E} := \{e^{(i)} \mid i \in \mathcal{I}\},$$
$$\mathcal{I} := \{1, 2, \dots, 12\}$$

or simply by $i \in \mathcal{I}$ if the meaning is clear from the context. The transformation strains involve four lattice parameters α, β, ε and δ. These have been chosen such that $\varepsilon > 0$ and $\delta > 0$. Typical lattice parameters are listed in Table 5.2. Note that $\operatorname{Tr} e = 2\alpha + \beta$ for $e \in \mathcal{E}$; thus $\mathcal{E} \subset \mathcal{S}^{3\times 3}_{2\alpha+\beta}$.

Compatibility. Compatibility and incompatibility between the transformation strains is of critical importance to us. A simple calculation [CSa, Compatibility.nb] shows that for $e, f \in \mathcal{E}$,

$$\det(e - f) \in \left\{0, \pm 4\varepsilon\left((\alpha-\beta)\delta + \varepsilon^2 - \delta^2\right)\right\}, \tag{5.1}$$

which gives the compatibility/incompatibility of the strains by Lemma 2.2.

Note that if the material parameters happen to be such that $(\alpha-\beta)\delta + \varepsilon^2 - \delta^2 = 0$ then all strains in $\mathcal{E}$ are pairwise compatible. Then by Lemma 2.10, $\mathcal{L}(\mathcal{E}) = \mathcal{C}(\mathcal{E})$. (In this case the material is able to form many more twins than usual [PZ98].)

Pairs of compatible and incompatible transformation strains in $\mathcal{E}$ are listed in Table 5.3. Here and henceforth (including in Mathematica calculations) we

i	$e^{(i)}$	i	$e^{(i)}$	i	$e^{(i)}$	i	$e^{(i)}$
1	$\begin{pmatrix} \alpha & \delta & \varepsilon \\ \delta & \alpha & \varepsilon \\ \varepsilon & \varepsilon & \beta \end{pmatrix}$	2	$\begin{pmatrix} \alpha & \delta & -\varepsilon \\ \delta & \alpha & -\varepsilon \\ -\varepsilon & -\varepsilon & \beta \end{pmatrix}$	3	$\begin{pmatrix} \alpha & -\delta & -\varepsilon \\ -\delta & \alpha & \varepsilon \\ -\varepsilon & \varepsilon & \beta \end{pmatrix}$	4	$\begin{pmatrix} \alpha & -\delta & \varepsilon \\ -\delta & \alpha & -\varepsilon \\ \varepsilon & -\varepsilon & \beta \end{pmatrix}$
5	$\begin{pmatrix} \alpha & \varepsilon & \delta \\ \varepsilon & \beta & \varepsilon \\ \delta & \varepsilon & \alpha \end{pmatrix}$	6	$\begin{pmatrix} \alpha & -\varepsilon & \delta \\ -\varepsilon & \beta & -\varepsilon \\ \delta & -\varepsilon & \alpha \end{pmatrix}$	7	$\begin{pmatrix} \alpha & -\varepsilon & -\delta \\ -\varepsilon & \beta & \varepsilon \\ -\delta & \varepsilon & \alpha \end{pmatrix}$	8	$\begin{pmatrix} \alpha & \varepsilon & -\delta \\ \varepsilon & \beta & -\varepsilon \\ -\delta & -\varepsilon & \alpha \end{pmatrix}$
9	$\begin{pmatrix} \beta & \varepsilon & \varepsilon \\ \varepsilon & \alpha & \delta \\ \varepsilon & \delta & \alpha \end{pmatrix}$	10	$\begin{pmatrix} \beta & -\varepsilon & -\varepsilon \\ -\varepsilon & \alpha & \delta \\ -\varepsilon & \delta & \alpha \end{pmatrix}$	11	$\begin{pmatrix} \beta & -\varepsilon & \varepsilon \\ -\varepsilon & \alpha & -\delta \\ \varepsilon & -\delta & \alpha \end{pmatrix}$	12	$\begin{pmatrix} \beta & \varepsilon & -\varepsilon \\ \varepsilon & \alpha & -\delta \\ -\varepsilon & -\delta & \alpha \end{pmatrix}$

Table 5.1: The transformation strains of the twelve variants of monoclinic-I martensite, cf. eg. [BK97, Table 1, p. 119].

	α	β	δ	ε	Reference
NiTi	0.0243	-0.0437	0.0580	0.0427	[OSS71, KS81, HS99]
CuZr	0.0348	0.0229	0.1067	0.0929	[SS98a, SS98b]
TiNiCu	0.0232	-0.0410	0.0532	0.0395	[NSNS90]

Table 5.2: Typical lattice parameters for monoclinic-I martensite, cf. eg. [SB97, Table 2, p. 5459] and [Bha03, p. 55 and 184].

assume that $(\alpha - \beta)\delta + \varepsilon^2 - \delta^2 \neq 0$ and, more generally, that the lattice parameters are generic. We also assume that $\alpha \neq \beta$, the (mathematical) reason for this will become clear in Section 6. There we will also see that the case $\varepsilon = \delta$ is special so we shall specifically consider this possibility.

i	$\det(e^{(\cdot)} - e^{(i)}) = 0$	$\det(e^{(\cdot)} - e^{(i)}) \gneqq 0$	$\det(e^{(\cdot)} - e^{(i)}) \lneqq 0$
1	2, 3, 4, 5, 7, 9, 11	8, 12	6, 10
2	1, 3, 4, 6, 8, 10, 12	5, 9	7, 11
3	1, 2, 4, 5, 7, 10, 12	6, 11	8, 9
4	1, 2, 3, 6, 8, 9, 11	7, 10	5, 12
5	1, 3, 6, 7, 8, 9, 12	4, 11	2, 10
6	2, 4, 5, 7, 8, 10, 11	1, 9	3, 12
7	1, 3, 5, 6, 8, 10, 11	2, 12	4, 9
8	2, 4, 5, 6, 7, 9, 12	3, 10	1, 11
9	1, 4, 5, 8, 10, 11, 12	3, 7	2, 6
10	2, 3, 6, 7, 9, 11, 12	1, 5	4, 8
11	1, 4, 6, 7, 9, 10, 12	2, 8	3, 5
12	2, 3, 5, 8, 9, 10, 11	4, 6	1, 7

Table 5.3: Compatible and incompatible transformation strains [CSa, Compatibility.nb]. The signs in the second and third columns depend on the material parameters; the sign in the third column is opposite to the one in the second.

Distances. Also of importance is the distance between the transformation strains [CSa, Distances.nb]:

Observation 5.1 Every pair of incompatible transformation strains is equidistant: For $e, f \in \mathcal{E}$ with $e \not\| f$,

$$\|e - f\|^2 = 2(\alpha - \beta)^2 + 4\delta^2 + 12\epsilon^2. \tag{5.2a}$$

Remark 5.13 sheds more light on this.

However for pairs of compatible transformation strains the situation is more complex: For $e, f \in \mathcal{E}$ with $e \| f$ and $e \neq f$,

$$\|e - f\|^2 \in \left\{16\varepsilon^2, 8(\delta^2 + \varepsilon^2), 2(\alpha - \beta)^2 + 4(\delta - \varepsilon)^2, 2(\alpha - \beta)^2 + 4(\delta + \varepsilon)^2\right\}. \tag{5.2b}$$

Table 5.4 presents the full picture. (See also Remark 5.11.)

We exclude (until Section 8) the special case $\varepsilon = \delta$ for which, for $e, f \in \mathcal{E}$ with $e \neq f$,

$$\|e - f\|^2 \in \left\{16\varepsilon^2, 2(\alpha - \beta)^2, 2(\alpha - \beta)^2 + 16\varepsilon^2\right\}.$$

Note that in this case, we cannot anymore distinguish between compatible and incompatible strains on the basis of the distance between them.

i	$\|e^{(\cdot)} - e^{(i)}\|^2 = 16\varepsilon^2$	$\|e^{(\cdot)} - e^{(i)}\|^2 = 8(\delta^2 + \varepsilon^2)$	$\|e^{(\cdot)} - e^{(i)}\|^2 = 2(\alpha - \beta)^2 + 4(\delta - \varepsilon)^2$	$\|e^{(\cdot)} - e^{(i)}\|^2 = 2(\alpha - \beta)^2 + 4(\delta + \varepsilon)^2$
1	2	3, 4	5, 9	7, 11
2	1	3, 4	8, 12	6, 10
3	4	1, 2	7, 10	5, 12
4	3	1, 2	6, 11	8, 9
5	6	7, 8	1, 9	3, 12
6	5	7, 8	4, 11	2, 10
7	8	5, 6	3, 10	1, 11
8	7	5, 6	2, 12	4, 9
9	10	11, 12	1, 5	4, 8
10	9	11, 12	3, 7	2, 6
11	12	9, 10	4, 6	1, 7
12	11	9, 10	2, 8	3, 5

Table 5.4: Distances between compatible transformation strains [CSa, Distances.nb].

Symmetry. Now that we have knowledge of the compatibilities and the distances between the transformation strains we are ready to analyse the symmetry between them:

Definition 5.2 (Symmetry and symmetry group)

1. A map $\tau\colon \mathcal{E} \to \mathcal{E}$ is a symmetry of $\mathcal{E}$ if it preserves distance and compatibility in $\mathcal{E}$. That is, $\forall e, f \in \mathcal{E}$,

$$\|e - f\| = \|\tau e - \tau f\|,$$
$$\det(e - f) = \pm \det(\tau e - \tau f).$$

A symmetry group of $\mathcal{E}$ is a group of symmetries of $\mathcal{E}$.

2. Let $n \in \mathcal{I} \setminus \{1\}$ and $\mathcal{E}_n$ be a set of subsets of $\mathcal{E}$, all with cardinality n. That is,
$$\mathcal{E}_n \subset \{S \subset \mathcal{E} \mid \#S = n\}\,.$$
A map $\tau\colon \mathcal{E}_n \to \mathcal{E}_n$ is a symmetry of $\mathcal{E}_n$ if it preserves distance and compatibility in $\mathcal{E}_n$. That is, $\forall S \in \mathcal{E}_n$, $\forall e, f \in S$,
$$\begin{aligned} \|e - f\| &= \|\tau e - \tau f\|, \\ \det(e - f) &= \pm \det(\tau e - \tau f). \end{aligned}$$
A symmetry group of $\mathcal{E}_n$ is a group of symmetries of $\mathcal{E}_n$.

There are four sets that are of interest to us here. These are: (i) $\mathcal{E}$ itself, (ii) $\mathcal{E}^2_{|||}$, the set of pairs of compatible transformation strains, (iii) $\mathcal{E}^2_{\not|\not|}$, the set of pairs of incompatible transformation strains, and (iv) $\mathcal{E}^3_{\not|\not|}$, the set of three-tuples of incompatible transformation strains:
$$\begin{aligned} \mathcal{E}^2_{|||} &:= \{\{e, f\} \mid e, f \in \mathcal{E},\ e \neq f,\ e \,|||\, f\}\,, \\ \mathcal{E}^2_{\not|\not|} &:= \{\{e, f\} \mid e, f \in \mathcal{E},\ e \not|\not| f\}\,, \\ \mathcal{E}^3_{\not|\not|} &:= \{\{e, f, g\} \mid e, f, g \in \mathcal{E},\ e \not|\not| f \not|\not| g \not|\not| e\}\,. \end{aligned}$$
We characterise the symmetry of $\mathcal{E}$ and $\mathcal{E}^2_{|||}$ in Lemma 5.10 and those of $\mathcal{E}^2_{\not|\not|}$ and $\mathcal{E}^3_{\not|\not|}$ in Lemma 5.12 below. In order to do so we begin with some observations. For further investigation of these sets see [CSb].

Observation 5.3 (S_4 is a symmetry group of $\mathcal{E}$) Since the transformation strains in $\mathcal{E}$ are obtained through a phase transformation from a cubic crystal, S_4, the group of rotational symmetries of a cube, is a symmetry group of $\mathcal{E}$.

This group and its action on $\mathcal{E}$ can be generated as follows: Let R_1, R_2 and R_3 be anticlockwise rotations of $\frac{\pi}{2}$ about the coordinate axes:
$$R_1 = \begin{pmatrix} 1 & 0 & 0 \\ 0 & 0 & -1 \\ 0 & 1 & 0 \end{pmatrix}, \qquad R_2 = \begin{pmatrix} 0 & 0 & 1 \\ 0 & 1 & 0 \\ -1 & 0 & 0 \end{pmatrix}, \qquad R_3 = \begin{pmatrix} 0 & -1 & 0 \\ 1 & 0 & 0 \\ 0 & 0 & 1 \end{pmatrix}.$$
For $i = 1, 2, 3$, let r_i be the map
$$\mathcal{S}^{3\times 3} \ni e \mapsto r_i e := R_i e R_i^T. \tag{5.3}$$
It is immediate that these are distance and determinant (and thus, compatibility) preserving: $\forall i = 1, 2, 3$, $\forall e, f \in \mathcal{E}$,
$$\|e - f\| = \|r_i e - r_i f\|, \tag{5.4a}$$
$$\det(e - f) = \det(r_i e - r_i f). \tag{5.4b}$$
Then $\{r_1, r_2, r_3\}$ generates S_4. (In fact any two of r_1, r_2, r_3 generate S_4 but it is convenient to retain all three.) The action of S_4 on $\mathcal{E}$ is listed, eg. in [HS99,

i	1	2	3	4	5	6	7	8	9	10	11	12
$r_1 i$	6	5	8	7	4	3	2	1	11	12	10	9
$r_2 i$	12	11	9	10	8	7	5	6	2	1	3	4
$r_3 i$	3	4	2	1	10	9	12	11	7	8	5	6

Table 5.5: The action of r_1, r_2, r_3 on $\mathcal{I}$.

Table 1, p. 2607] but their numbering of the transformation strains is different from ours.

S_4 is isomorphic to a group of permutations on $\mathcal{I}$. We denote this group too by S_4; the images of r_1, r_2, r_3 under this isomorphism are also denoted by r_1, r_2, r_3. Table 5.5 lists the action of r_1, r_2, r_3 on $\mathcal{I}$ [CSa, Symmetry.nb].

Remark 5.4 Since S_4 is the group of rotational symmetries of a cube, it is natural and convenient to identify $\mathcal{E}$ (and $\mathcal{I}$) with the edges of a cube as shown in Figure 5.1. (We could also have identified them with the diagonals of the faces.) Then r_1, r_2, r_3 are anticlockwise rotations of $\frac{\pi}{2}$ along an axis perpendicular to the face of the cube and passing through its centre.

From Table 5.3 we note that the four edges with which an edge is incompatible are precisely the four edges with which it shares a vertex. Thus,

1. The 24 elements of $\mathcal{E}^2_{/\!/}$ can be identified with the 24 corners of the faces of a cube, and
2. The 8 elements of $\mathcal{E}^3_{/\!/}$ can be identified with the 8 corners of a cube.

Our next task is to show that $\mathcal{E}$ does not have the reflection symmetries of a cube. We will accomplish this in Observation 5.9 below.

Definition 5.5 (Inversion) Let r_0 be the permutation on $\mathcal{I}$ which interchanges 1 and 2, 3 and 4, 5 and 6, 7 and 8, 9 and 10, and 11 and 12.

As can be seen from Figure 5.1, r_0 is an inversion (reflection through the centre) of the cube. This immediately shows both that $r_0 \notin S_4$ and that $\{r_0, r_1, r_2, r_3\}$ generates $S_4 \times C_2$, the group of symmetries of a cube (including reflections).

Remark 5.6 The permutation r_0 corresponds to replacing ε with $-\varepsilon$ in the transformation strains (cf. Table 5.1).

Observation 5.7 Unlike r_1, r_2 and r_3, r_0 cannot be identified with a linear operator on $\mathcal{S}^{3\times 3}_{2\alpha+\beta}$.

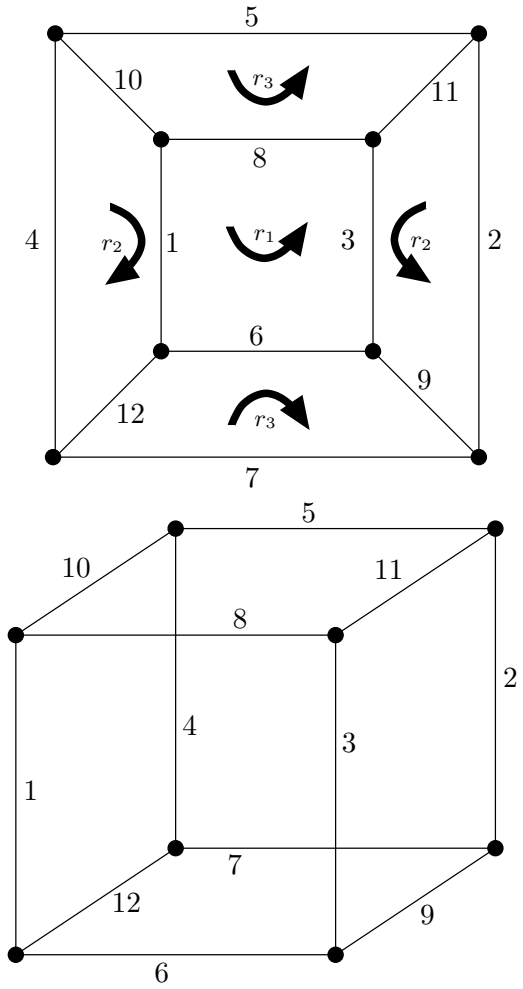


Fig. 5.1: The oriented cube representing the symmetries of $\mathcal{E}$ [CSa, Symmetry.nb].

Proof Assume, on the contrary, that there exists $\mathcal{L}\colon \mathcal{S}^{3\times 3}_{2\alpha+\beta} \to \mathcal{S}^{3\times 3}_{2\alpha+\beta}$, linear, such that $\forall i \in \mathcal{I}$, $\mathcal{L}e^{(i)} = e^{(r_0 i)}$. Then,

$$\mathcal{L}\left(e^{(1)}+e^{(2)}+e^{(3)}+e^{(4)}\right) = e^{(1)}+e^{(2)}+e^{(3)}+e^{(4)}$$
$$\implies \mathcal{L}\begin{pmatrix}\alpha & 0 & 0\\ 0 & \alpha & 0\\ 0 & 0 & \beta\end{pmatrix} = \begin{pmatrix}\alpha & 0 & 0\\ 0 & \alpha & 0\\ 0 & 0 & \beta\end{pmatrix},$$
$$\mathcal{L}\left(e^{(5)}+e^{(6)}+e^{(7)}+e^{(8)}\right) = e^{(5)}+e^{(6)}+e^{(7)}+e^{(8)}$$
$$\implies \mathcal{L}\begin{pmatrix}\alpha & 0 & 0\\ 0 & \beta & 0\\ 0 & 0 & \alpha\end{pmatrix} = \begin{pmatrix}\alpha & 0 & 0\\ 0 & \beta & 0\\ 0 & 0 & \alpha\end{pmatrix},$$
$$\mathcal{L}\left(e^{(9)}+e^{(10)}+e^{(11)}+e^{(12)}\right) = e^{(9)}+e^{(10)}+e^{(11)}+e^{(12)}$$
$$\implies \mathcal{L}\begin{pmatrix}\beta & 0 & 0\\ 0 & \alpha & 0\\ 0 & 0 & \alpha\end{pmatrix} = \begin{pmatrix}\beta & 0 & 0\\ 0 & \alpha & 0\\ 0 & 0 & \alpha\end{pmatrix}.$$

Thus (i) $\mathcal{L}$ is an identity on the diagonal components of $\mathcal{S}^{3\times3}_{2\alpha+\beta}$. Moreover

$$\mathcal{L}\left(e^{(1)}+e^{(3)}\right)=e^{(2)}+e^{(4)} \implies \mathcal{L}\begin{pmatrix}\alpha&0&0\\0&\alpha&\varepsilon\\0&\varepsilon&\beta\end{pmatrix}=\begin{pmatrix}\alpha&0&0\\0&\alpha&-\varepsilon\\0&-\varepsilon&\beta\end{pmatrix},$$

$$\mathcal{L}\left(e^{(5)}+e^{(8)}\right)=e^{(6)}+e^{(7)} \implies \mathcal{L}\begin{pmatrix}\alpha&\varepsilon&0\\\varepsilon&\beta&0\\0&0&\alpha\end{pmatrix}=\begin{pmatrix}\alpha&-\varepsilon&0\\-\varepsilon&\beta&0\\0&0&\alpha\end{pmatrix},$$

$$\mathcal{L}\left(e^{(9)}+e^{(11)}\right)=e^{(10)}+e^{(12)} \implies \mathcal{L}\begin{pmatrix}\beta&0&\varepsilon\\0&\alpha&0\\\varepsilon&0&\alpha\end{pmatrix}=\begin{pmatrix}\beta&0&-\varepsilon\\0&\alpha&0\\-\varepsilon&0&\alpha\end{pmatrix}.$$

Thus (ii) $\mathcal{L}$ is a negative of the identity on the off-diagonal components of $\mathcal{S}^{3\times3}_{2\alpha+\beta}$.

It is easy to check that (i) and (ii) are contradictory, eg. $\mathcal{L}e^{(1)}=e^{(2)}$.

Now we address the question of whether r_0 is a symmetry of $\mathcal{E}$:

Observation 5.8 (Inversions preserve compatibility) As can be verified [CSa, Symmetry.nb] from Table 5.3 and (5.1), r_0 is compatibility preserving: $\forall e, f \in \mathcal{E}$,

$$\det(e-f)=-\det(r_0e-r_0f).$$

Observation 5.9 (Effect of inversions on distance) From Observation 5.1 and Remark 5.6 it follows that r_0 is distance-preserving on pairs of incompatible transformation strains. However it is distance-preserving only on some pairs of compatible transformation strains: For $e, f \in \mathcal{E}$,

$$\|e-f\|^2=\|r_0e-r_0f\|^2 \qquad \iff \qquad \|e-f\|^2\neq 2(\alpha-\beta)^2+4(\delta\pm\varepsilon)^2. \quad (5.5)$$

This is easy to verify in view of the following: Let $e, f \in \mathcal{E}$ with $e \mid\mid\mid f$. Then,

$$\|e-f\|^2=\begin{cases}16\varepsilon^2 & \text{if } e=r_0f,\\ 8\delta^2+8\varepsilon^2 & \text{if } \exists i\in\{1,2,3\},\ e=r_if,\\ 2(\alpha-\beta)^2+4(\delta\pm\varepsilon)^2 & \text{else.}\end{cases} \quad (5.6)$$

(The middle case corresponds to parallel edges of the cube that share a face.)

Thus r_0 is not a symmetry of $\mathcal{E}$ nor is it a symmetry of $\mathcal{E}^2_{|||}$. In the light of Observation 5.3 we conclude that $\mathcal{E}$ and $\mathcal{E}^2_{|||}$ have the rotation symmetries of a cube but not its reflection symmetries:

Lemma 5.10 *S_4 is a symmetry group of $\mathcal{E}$ and $\mathcal{E}^2_{|||}$, whereas $S_4\times C_2$ is not a symmetry group of $\mathcal{E}$ or $\mathcal{E}^2_{|||}$.*

Remark 5.11 From (5.2b) we deduce that the orbits of S_4 partition $\mathcal{E}^2_{|||}$ into four equivalence classes. (Equation (5.6) relates this to the edges of a cube.)

Observations 5.1, 5.3 and 5.8 show that $\mathcal{E}^2_{\#}$ and $\mathcal{E}^3_{\#}$ have the symmetries of a cube:

Lemma 5.12 *$S_4 \times C_2$ is a symmetry group of $\mathcal{E}^2_{\#}$ and of $\mathcal{E}^3_{\#}$.*

Remark 5.13 From Remark 5.4(1) it is clear that $S_4 \times C_2$ (or indeed S_4) acts transitively on $\mathcal{E}^2_{\#}$, i.e., the orbit of any element of $\mathcal{E}^2_{\#}$ under $S_4 \times C_2$ equals $\mathcal{E}^2_{\#}$. This explains Observation 5.1. Likewise, from Remark 5.4(2) it is clear that $S_4 \times C_2$ (or indeed S_4) acts transitively on $\mathcal{E}^3_{\#}$.

6 The convex polytope formed by the transformation strains

In this section we study $\mathcal{C}(\mathcal{E})$, the convex hull of $\mathcal{E}$, which is a five-dimensional polytope [CSa, Dimension.nb], when, as we have assumed, $\alpha \neq \beta$ (otherwise it is a three-dimensional polytope). We are interested in the *facets* of $\mathcal{C}(\mathcal{E})$. However the *vertices* and *edges* of $\mathcal{C}(\mathcal{E})$ are also of interest and we begin with them.

For convenience we set $\Lambda = \{\lambda \in [0,1]^{12},\ \sum_{i=1}^{12} \lambda_i = 1\}$. The following linear functionals will be helpful in studying $\mathcal{C}(\mathcal{E})$:

Definition 6.1 The linear functionals $H_i \colon \mathcal{S}^{3\times 3} \to \mathbb{R}$, $i = 0, 1, 2, 3$, are defined by

$$\begin{aligned} H_0\, e &= -e_{12} - e_{23} - e_{31}, \\ H_1\, e = H_0\, r_1 e &= -e_{12} + e_{23} + e_{31}, \\ H_2\, e = H_0\, r_2 e &= e_{12} - e_{23} + e_{31}, \\ H_3\, e = H_0\, r_3 e &= e_{12} + e_{23} - e_{31}; \end{aligned}$$

and $H_{ij} \colon \mathcal{S}^{3\times 3} \to \mathbb{R}$, $i, j = 1, 2, 3$, by

$$H_{ij}\, e = e_{ij},$$

where e_{ij} denotes the (i, j)-component of the matrix e.

For the convenience of the reader we summarise the images of the transformation strains under the functionals H_i, $i = 0, 1, 2, 3$, in Table 6.1. We also list the extremisers of these functionals; note that the extremisers when $\varepsilon = \delta$ are the union of the extremisers when $\varepsilon < \delta$ and when $\varepsilon > \delta$.

Vertices. The *vertices* of $\mathcal{C}(\mathcal{E})$ are the transformation strains:

Lemma 6.2 *The set of vertices of $\mathcal{C}(\mathcal{E})$ is $\mathcal{E}$.*

Proof We show this explicitly for $e^{(1)}$, the proof for the other vertices follows from symmetry.

i	$H_0\, e^{(i)}$	$H_1\, e^{(i)}$	$H_2\, e^{(i)}$	$H_3\, e^{(i)}$
1	$-\delta-2\varepsilon$	$-\delta+2\varepsilon$	δ	δ
2	$-\delta+2\varepsilon$	$-\delta-2\varepsilon$	δ	δ
3	δ	δ	$-\delta-2\varepsilon$	$-\delta+2\varepsilon$
4	δ	δ	$-\delta+2\varepsilon$	$-\delta-2\varepsilon$
5	$-\delta-2\varepsilon$	δ	δ	$-\delta+2\varepsilon$
6	$-\delta+2\varepsilon$	δ	δ	$-\delta-2\varepsilon$
7	δ	$-\delta+2\varepsilon$	$-\delta-2\varepsilon$	δ
8	δ	$-\delta-2\varepsilon$	$-\delta+2\varepsilon$	δ
9	$-\delta-2\varepsilon$	δ	$-\delta+2\varepsilon$	δ
10	$-\delta+2\varepsilon$	δ	$-\delta-2\varepsilon$	δ
11	δ	$-\delta+2\varepsilon$	δ	$-\delta-2\varepsilon$
12	δ	$-\delta-2\varepsilon$	δ	$-\delta+2\varepsilon$

	$i\mapsto H_0\, e^{(i)}$	$i\mapsto H_1\, e^{(i)}$	$i\mapsto H_2\, e^{(i)}$	$i\mapsto H_3\, e^{(i)}$
minimisers	1,5,9	2,8,12	3,7,10	4,6,11

Maximisers	$i\mapsto H_0\, e^{(i)}$	$i\mapsto H_1\, e^{(i)}$	$i\mapsto H_2\, e^{(i)}$	$i\mapsto H_3\, e^{(i)}$
When $\varepsilon<\delta$	3,4,7,8,11,12	3,4,5,6,9,10	1,2,5,6,11,12	1,2,7,8,9,10
When $\varepsilon=\delta$	$\mathcal{I}\setminus\{1,5,9\}$	$\mathcal{I}\setminus\{2,8,12\}$	$\mathcal{I}\setminus\{3,7,10\}$	$\mathcal{I}\setminus\{4,6,11\}$
When $\varepsilon>\delta$	2,6,10	1,7,11	4,8,9	3,5,12

Table 6.1: The images of the transformation strains under the linear functionals H_i, $i=0,1,2,3$, along with their extremisers [CSa, Linear_Functionals.nb].

Let $\lambda\in\Lambda$ such that $e^{(1)}=\sum_{i=1}^{12}\lambda_i e^{(i)}$. Then,

$$\beta=H_{33}e^{(1)}=\sum_{i=1}^{12}\lambda_i H_{33}e^{(i)}=\sum_{i=1}^{4}\lambda_i\beta+\sum_{i=5}^{12}\lambda_i\alpha,$$

from which we conclude that $\lambda_i=0$ for $i=5,\dots,12$ and thus $e^{(1)}=\sum_{i=1}^{4}\lambda_i e^{(i)}$. Now, using H_0 we obtain

$$-\delta-2\epsilon=H_0e^{(1)}=\sum_{i=1}^{4}\lambda_i H_0e^{(i)}.$$

Since $\varepsilon,\delta>0$ it is easy to see (cf. Table 6.1) that $\lambda_1=1$ and $\lambda_i=0$, $i=2,3,4$. We conclude that $e^{(1)}$ is a vertex.

In the interest of brevity in future proofs of extremality of subsets we will only name the relevant family of four-dimensional hyperplanes, eg. for the above lemma we would say that this follows from H_{33} and H_0.

Edges. Contrary to what we are used to in two and three dimensions (see Remark 6.4 below), the convex hull of *every* pair of vertices is an edge of $\mathcal{C}(\mathcal{E})$:

Lemma 6.3 *The set of edges of* $\mathcal{C}(\mathcal{E})$ *is* $\{[e,f]\mid e,f\in\mathcal{E}\}$.

Henceforth, a *compatible edge* is the convex hull of a pair of compatible vertices, and an *incompatible edge* is the convex hull of a pair of incompatible vertices.

We prove Lemma 6.3 here except for incompatible edges when $\varepsilon > \delta$. In Remark 6.10 we present a Mathematica-aided proof which is valid for $\varepsilon \neq \delta$.

Proof (for compatible edges and, when $\varepsilon \leqslant \delta$, for incompatible edges) By symmetry it suffices to prove that the eleven edges $[e^{(1)}, e^{(i)}]$, $i \in \mathcal{I} \setminus \{1\}$, are extremal.

This is easy to verify for the compatible edges: For example, H_{33} and H_{12} show that $[e^{(1)}, e^{(2)}]$ is extremal. The proof for the other compatible edges (with $e^{(1)}$ as a vertex) is similar.

We now turn to the incompatible edges, for example $[e^{(1)}, e^{(6)}]$. Let $\mu \in [0,1]$ and $\lambda \in \Lambda$ such that

$$\mu e^{(1)} + (1-\mu)e^{(6)} = \sum_{i=1}^{12} \lambda_i e^{(i)}.$$

Consider first the case $\varepsilon < \delta$. Then H_{11} and H_2 show that in fact

$$\mu e^{(1)} + (1-\mu)e^{(6)} = \sum_{i \in \{1,2,5,6\}} \lambda_i e^{(i)}.$$

However $\dim \operatorname{aff} \operatorname{span}\{e^{(1)}, e^{(2)}, e^{(5)}, e^{(6)}\} = 3$ [CSa, Dimension_Calculations.nb] and thus
$\mathcal{C}(\{e^{(1)}, e^{(2)}, e^{(5)}, e^{(6)}\})$ is a three-dimensional tetrahedron. It follows that $\lambda_5 = \lambda_2 = 0$ and thus $[e^{(1)}, e^{(6)}]$ is extremal.

Next consider the case $\varepsilon = \delta$. Then H_{11}, H_{13}, H_1 and H_2 show that in fact

$$\mu e^{(1)} + (1-\mu)e^{(6)} = \sum_{i \in \{1,5,6\}} \lambda_i e^{(i)}.$$

However $\dim \operatorname{aff} \operatorname{span}\{e^{(1)}, e^{(5)}, e^{(6)}\} = 2$ [CSa, Dimension_Calculations.nb] and thus
$\mathcal{C}(\{e^{(1)}, e^{(5)}, e^{(6)}\})$ is a triangle. It follows that $\lambda_5 = 0$ and thus $[e^{(1)}, e^{(6)}]$ is extremal.

The extremality of the other incompatible edges (with $e^{(1)}$ as a vertex) follows from symmetry.

Remark 6.4 In dimensions less than four the only polytopes for which the convex hull of every pair of vertices is an edge are the n-tetrahedra (line segments, triangles and tetrahedra in dimensions one, two and three, respectively). However for every $n > 3$ and every $d > n$ there exists an n-dimensional convex polytope with d vertices for which the convex hull of every pair of vertices is extremal. See, eg. [Brø82, Section 13], [Ewa96, Section 3] or [Zie94, Corollary 0.8].

The facets of $\mathcal{C}(\mathcal{E})$. The algorithm we use to determine the facets of $\mathcal{C}(\mathcal{E})$ is as follows [CSa, Faceting.nb]. It assumes that the affine span of the set is five-dimensional, that the cardinality of the set is small and thus that computational efficiency is not a consideration.

Algorithm 6.5

1. *First we form a set of all four-dimensional tetrahedra with vertices in* $\mathcal{E}$ *as follows:*
 (a) *Pick all five-tuples from* $\mathcal{E}$*:*
 $$\{S \subset \mathcal{E} \mid \#S = 5\}.$$
 (b) *Discard those five-tuples whose affine span is not four dimensional:*
 $$\mathcal{G}_1 := \{S \subset \mathcal{E} \mid \#S = 5, \dim \operatorname{aff} \operatorname{span}(S) = 4\}.$$
2. *Of these tetrahedra we discard those whose convex hull is not contained in* $\partial\mathcal{C}(\mathcal{E})$. *We do this as follows:*
 (a) *Let* $\mathcal{G}_2 = \mathcal{G}_1$.
 (b) *Pick* $S \in \mathcal{G}_2$.
 (c) *Translate the origin to some* $e \in S$. *(The next two steps are carried out in this co-ordinate system.)*
 (d) *Compute a normal* $n \in \mathcal{S}^{3\times 3}_{2\alpha+\beta}$ *to* $\operatorname{aff} \operatorname{span}(S)$.
 (e) *If* $\langle n, e\rangle$ *has the same sign for all* $e \in \mathcal{E}\backslash S$ *then* $\mathcal{C}(S) \subset \partial\mathcal{C}(\mathcal{E})$. *Otherwise remove* S *from* G_2
 (f) *Repeat steps* (2b) *to* (2e) *till all tetrahedra in* $\mathcal{G}_2$ *have been tested.*
 We now obtain
 $$\mathcal{G}_2 = \{S \subset \mathcal{E} \mid \#S = 5, \dim \operatorname{aff} \operatorname{span}(S) = 4, \mathcal{C}(S) \subset \partial\mathcal{C}(\mathcal{E})\}.$$
 This is the set of all four-dimensional tetrahedra (with vertices in $\mathcal{E}$*) whose union is* $\partial\mathcal{C}(\mathcal{E})$.
3. *The final step is to form the facets of* $\mathcal{C}(\mathcal{E})$ *by judiciously taking unions of sets in* $\mathcal{G}_2$ *as follows:*
 (a) *Let* $\mathcal{G}_3 = \mathcal{G}_2$.
 (b) *Pick* $S_1, S_2 \in \mathcal{G}_3$.
 (c) *If* $\dim \operatorname{aff} \operatorname{span}(S_1 \cup S_2) = 4$ *then* S_1 *and* S_2 *are parts of the same facet. In* $\mathcal{G}_3$*, replace* S_1 *and* S_2 *by* $S_1 \cup S_2$.
 (d) *Repeat steps* (3b) *and* (3c) *until every union of sets in* G_3 *increases the dimension, i.e., until it is true that*
 $$\forall S_1, S_2 \in \mathcal{G}_3, \qquad \dim \operatorname{aff} \operatorname{span}(S_1 \cup S_2) = 4 \implies S_1 = S_2. \tag{6.1}$$
 This is the set of all the facets of $\mathcal{C}(\mathcal{E})$. *Note that it is a set of* n*-tuples where* $n \geqslant 5$.

The results of a Mathematica implementation of Algorithm 6.5 are summarised in Observations 6.6, 6.7 and 6.8 below. These reveal that the facet structure depends on whether $\varepsilon < \delta$, $\varepsilon = \delta$ or $\varepsilon > \delta$. All three possibilities are realisable in that there exist cubic-to-monoclinic-I phase transformations corresponding to each. (See, e.g., [Bha03, Fig. 4.3 and (4.11) on p. 52–53] for the relationship between ε, δ and the unit cells of the cubic and monoclinic lattices.) However, curiously $\varepsilon < \delta$ for all the monoclinic-I materials of which we are aware, cf. Table 5.2; we return to this point in Section 8.

In the observations below, each group of facets is the orbit under S_4 of any facet in it [CSa, Facet_Symmetry.nb]. Within each group the facets are listed in lexical order. Facets that occur for both $\varepsilon < \delta$ and $\varepsilon > \delta$ are shown in bold face.

Observation 6.6 (Monoclinic-Ia martensite, $\varepsilon < \delta$) When $\varepsilon < \delta$, the 25 four-dimensional facets of $\mathcal{C}(\mathcal{E})$ consist of the convex hulls of

1. 12 facets with 5 vertices each:

$$\begin{aligned}&\{1,2,3,7,10\},\ \{1,2,4,6,11\},\ \{1,3,4,5,9\},\ \{1,5,7,8,9\},\\ &\{1,5,9,11,12\},\ \{2,3,4,8,12\},\ \{2,5,6,8,12\},\ \{2,8,9,10,12\},\\ &\{3,5,6,7,10\},\ \{3,7,10,11,12\},\ \{4,6,7,8,11\},\ \{4,6,9,10,11\};\end{aligned}$$

2. 4 pairs of T_3s (see Section 7), each facet is invariant under r_0:

$$\{1,2,5,6,11,12\},\ \{1,2,7,8,9,10\},\ \{3,4,5,6,9,10\},\ \{3,4,7,8,11,12\} \tag{6.2}$$

3. 6 pairs of pairwise compatible three-tuples:

$$\begin{aligned}&\{\mathbf{1,2,5,8,9,12}\},\ \{\mathbf{1,3,5,7,9,10}\},\ \{\mathbf{1,4,5,6,9,11}\},\\ &\{\mathbf{2,3,7,8,10,12}\},\ \{\mathbf{2,4,6,8,11,12}\},\ \{\mathbf{3,4,6,7,10,11}\};\end{aligned}$$

4. 3 facets with 8 vertices each; each facet is invariant under r_0:

$$\{\mathbf{1,2,3,4,5,6,7,8}\},\ \{\mathbf{1,2,3,4,9,10,11,12}\},\ \{\mathbf{5,6,7,8,9,10,11,12}\}. \tag{6.3}$$

Observation 6.7 ($\varepsilon = \delta$) When $\varepsilon = \delta$, the 7 four-dimensional facets of $\mathcal{C}(\mathcal{E})$ consist of the convex hulls of

1. 4 facets with 9 vertices each:

$$\begin{aligned}&\{1,2,3,5,7,8,9,10,12\},\ \{1,2,4,5,6,8,9,11,12\},\\ &\{1,3,4,5,6,7,9,10,11\},\ \{2,3,4,6,7,8,10,11,12\};\end{aligned} \tag{6.4}$$

2. 3 facets with 8 vertices each; each facet is invariant under r_0:

$$\{\mathbf{1,2,3,4,5,6,7,8}\},\ \{\mathbf{1,2,3,4,9,10,11,12}\},\ \{\mathbf{5,6,7,8,9,10,11,12}\}. \tag{6.3}$$

Observation 6.8 (Monoclinic-Ib martensite, $\varepsilon > \delta$) When $\varepsilon > \delta$, the 33 four-dimensional facets of $\mathcal{C}(\mathcal{E})$ consist of the convex hulls of

1. 12 facets which are the images under r_0 of the five-vertex facets that occur when $\varepsilon < \delta$:

$$\{1,2,3,5,12\},\ \{1,2,4,8,9\},\ \{1,3,4,7,11\},\ \{1,5,6,7,11\},$$
$$\{1,7,9,10,11\},\ \{2,3,4,6,10\},\ \{2,6,7,8,10\},\ \{2,6,10,11,12\},$$
$$\{3,5,7,8,12\},\ \{3,5,9,10,12\},\ \{4,5,6,8,9\},\ \{4,8,9,11,12\};$$

2. 12 other five vertex facets (together these are invariant under r_0):

$$\{1,3,5,9,12\},\ \{1,3,7,10,11\},\ \{1,4,5,8,9\},\ \{1,4,6,7,11\},$$
$$\{1,5,7,9,11\},\ \{2,3,5,8,12\},\ \{2,3,6,7,10\},\ \{2,4,6,10,11\},$$
$$\{2,4,8,9,12\},\ \{2,6,8,10,12\},\ \{3,5,7,10,12\},\ \{4,6,8,9,11\};$$

3. 6 pairs of pairwise compatible three-tuples:

$$\{\mathbf{1},\mathbf{2},\mathbf{5},\mathbf{8},\mathbf{9},\mathbf{12}\},\ \{\mathbf{1},\mathbf{3},\mathbf{5},\mathbf{7},\mathbf{9},\mathbf{10}\},\ \{\mathbf{1},\mathbf{4},\mathbf{5},\mathbf{6},\mathbf{9},\mathbf{11}\},$$
$$\{\mathbf{2},\mathbf{3},\mathbf{7},\mathbf{8},\mathbf{10},\mathbf{12}\},\ \{\mathbf{2},\mathbf{4},\mathbf{6},\mathbf{8},\mathbf{11},\mathbf{12}\},\ \{\mathbf{3},\mathbf{4},\mathbf{6},\mathbf{7},\mathbf{10},\mathbf{11}\};$$

4. 3 facets with 8 vertices each; each facet is invariant under r_0:

$$\{\mathbf{1},\mathbf{2},\mathbf{3},\mathbf{4},\mathbf{5},\mathbf{6},\mathbf{7},\mathbf{8}\},\ \{\mathbf{1},\mathbf{2},\mathbf{3},\mathbf{4},\mathbf{9},\mathbf{10},\mathbf{11},\mathbf{12}\},\ \{\mathbf{5},\mathbf{6},\mathbf{7},\mathbf{8},\mathbf{9},\mathbf{10},\mathbf{11},\mathbf{12}\}. \tag{6.3}$$

Remark 6.9 The extremality of facets that are invariant under r_0 can be verified as in the proof of Lemma 6.2: H_{11}, H_{22}, H_{33} show that the facets in (6.3) are extremal. H_i, $i = 0,1,2,3$, show that pairs of T_3s in (6.2) are extremal since $\varepsilon < \delta$ implies $-\delta - 2\varepsilon < -\delta < \delta - 2\varepsilon < \delta < \delta + 2\varepsilon$.

In addition H_i, $i = 0,1,2,3$, also show that the facets in (6.4) are extremal, cf. Table 6.1. For the remaining facets extremality can be verified through a computation of normals [CSa, Facet_Normal.nb].

Remark 6.10 (Proof of Lemma 6.3 when $\varepsilon \neq \delta$) Observations 6.6 and 6.8 lead to a proof of Lemma 6.3 when $\varepsilon \neq \delta$: Observe that every edge is shared by at least four facets. (This is particularly easy to check for the incompatible edges: Each incompatible edge is contained in precisely one facet from each group.) It follows that every edge is extremal (cf. eg. [Bar03, Chapter 6] or the other references listed in Section 2.2).

Remark 6.11 We remark that this phenomenon of polytope facet structure depending on lattice parameters is not possible for the other martensites (i.e., cubic-to-tetragonal, cubic-to-trigonal and cubic-to-orthorhombic) because they form n-tetrahedra (for $n = 2,3,5$, respectively) and thus their facet structure is fixed.

7 Non-laminate microstructures in $\mathcal{R}(\mathcal{E})$

In this section we use the results of the preceding sections to derive our central results about non-laminate microstructures in monoclinic-I martensite. These include T_3 microstructures formed by the strains in $\mathcal{E}$ (Section 7.1) and T_3 microstructures formed by the nodes of these T_3s (Section 7.2).

7.1 (Level-1) T_3s and related microstructures

As mentioned earlier there are precisely eight 3-tuples of pairwise incompatible vertices (cf. Table 5.3):

$$\mathcal{E}^3_{\not\parallel} = \Big\{\{e^{(1)},e^{(6)},e^{(12)}\},\ \{e^{(1)},e^{(8)},e^{(10)}\},\ \{e^{(2)},e^{(5)},e^{(11)}\},\ \{e^{(2)},e^{(7)},e^{(9)}\},\\ \{e^{(3)},e^{(6)},e^{(9)}\},\ \{e^{(3)},e^{(8)},e^{(11)}\},\ \{e^{(4)},e^{(5)},e^{(10)}\},\ \{e^{(4)},e^{(7)},e^{(12)}\}\Big\}.$$

Since

$$\operatorname{sign}\det(e^{(1)}-e^{(6)}) = \operatorname{sign}\det(e^{(6)}-e^{(12)}) = \operatorname{sign}\det(e^{(12)}-e^{(1)}) \neq 0$$

and likewise for the other 3-tuples, cf. Table 5.3, we obtain by Lemma 4.3 that each of these 3-tuples forms a T_3. (See also Remark 5.13.)

Let $v_{i,j,k} = \{e^{(i)},e^{(j)},e^{(k)}\} \in \mathcal{E}^3_{\not\parallel}$. We set

$$\tau_{i,j,k} = \mathcal{R}(v_{i,j,k}),$$
$$\mathcal{T} := \{\tau_{i,j,k} \mid v_{i,j,k} \in \mathcal{E}^3_{\not\parallel}\}.$$

For $\tau \in \mathcal{T}$ and $r \in S_4 \times C_2$ by $r\tau$ we mean the T_3 formed by the image under r of the vertices of τ. (The existence of such T_3s follows from $S_4 \times C_2$ being a symmetry group of $\mathcal{E}^3_{\not\parallel}$ as was shown in Lemma 5.12). The symmetry relations between the T_3s is illustrated in Figure 7.1. As we shall see (Example 7.3 below) each $\tau \in \mathcal{T}$ is specially related to $r_0\tau$; we refer to it as the *dual* of τ.

Before we proceed further we note that each of these eight T_3s is symmetric (Definition 4.6) and has distinct nodes (Definition 4.5). Moreover all eight T_3s are similar (Definition 4.8):

Lemma 7.1 *All T_3s in $\mathcal{T}$ are similar, and each is symmetric and has distinct nodes.*

Proof The symmetry of each T_3 and the similarity of all T_3s in $\mathcal{T}$ follow from Remark 5.13.

Now consider the nodes of $\tau_{1,8,10}$. Suppose, on the contrary, that $e_{1,8} = e_{8,10} = e_{10,1}$. (Here we use the notation of Section 4.) Then, by symmetry, the nodes coincide with the barycentre of the T_3 which is $\frac{1}{3}\left(e^{(1)}+e^{(8)}+e^{(10)}\right)$. However, an elementary calculation shows that this barycentre is incompatible with e_1, e_8 and e_{10} which is a contradiction (cf. Definition 4.1). Thus $\tau_{1,8,10}$ has distinct nodes and by symmetry this is true for all eight T_3s.

From Proposition 4.9 and symmetry it follows that the barycentre of each $v \in \mathcal{E}^3_{\not\parallel}$ is contained in $\mathcal{R}(v)$.

From Observations 6.6 and 6.7, when $\varepsilon \leqslant \delta$, each T_3 in $\mathcal{T}$ along with its dual is contained in a facet of $\mathcal{C}(\mathcal{E})$. In particular for each $\tau \in \mathcal{T}$, the symmetrised rank-one convex hull of $\tau \cup r_0\tau$ is contained in a facet of $\mathcal{C}(\mathcal{E})$ and is thus a part of the boundary of the symmetrised rank-one convex hull of $\mathcal{E}$:

$$\mathcal{R}(\tau \cup r_0\tau) \subset \partial\mathcal{R}(\mathcal{E}). \tag{7.1}$$

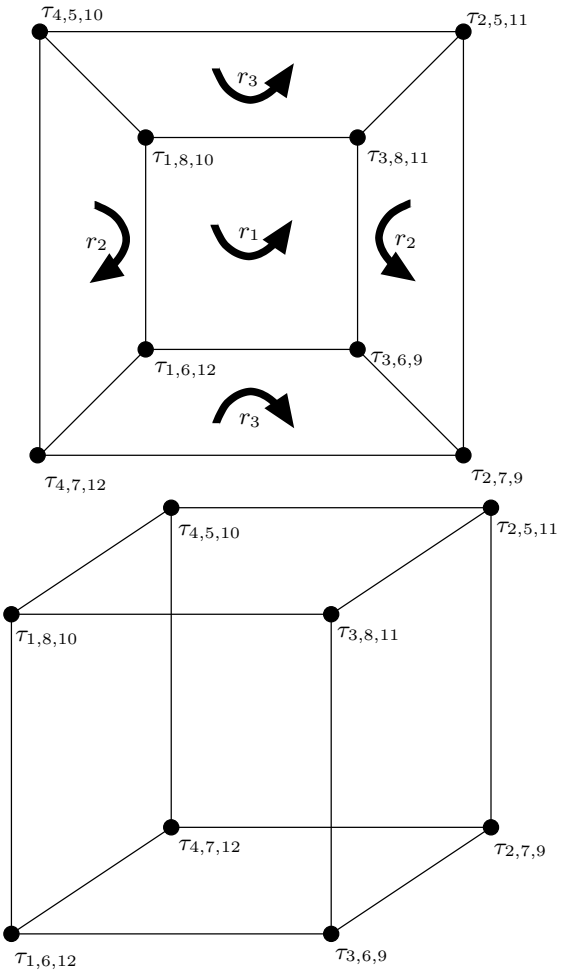


Fig. 7.1: The symmetry of the eight T_3s.

Example 7.3 below reveals that $\mathcal{R}(\tau \cup r_0\tau)$ is four dimensional and that each point in it can be attained by laminates of T_3 microstructures. In other words $\mathcal{R}(\tau \cup r_0\tau)$ contains a four-dimensional set of T_3s. Before we show this we first construct a three-dimensional set of T_3s which lies in $\partial\mathcal{R}(\mathcal{E})$ when $\varepsilon \leqslant \delta$.

Example 7.2 (A three-dimensional set of T_3s) Let $\tau \in \mathcal{T}$. From Table 5.3 the elements of $\mathcal{E}$ with which all the vertices of τ are compatible are precisely the vertices of $r_0\tau$. Following the construction introduced in Lemma 4.10, we construct a three-dimensional set of T_3s from τ and (any) one vertex from $r_0\tau$. There are three such continua of T_3s, one for each vertex of $r_o\tau$. Analogously there are three such sets constructed from $r_0\tau$ and the vertices of τ.

Note that this example shows that T_3s exist not only in $\mathcal{E}$ but also in $\mathcal{L}_1(\mathcal{E})\backslash\mathcal{E}$ since the vertices of almost all of the T_3s so constructed are themselves attained by a lamination of strains in $\mathcal{E}$. However in the next example the construction of T_3s precedes the construction of laminates:

Example 7.3 (A four-dimensional set of laminates of nodes of T_3s) From each $\tau \in \mathcal{T}$ and its dual we construct a four-dimensional set of laminates of nodes of T_3s. We do this explicitly for $\tau_{1,8,10}$ and its dual $\tau_{2,7,9}$; the construction for the other pairs is similar.

First we note that each point in one of these T_3s is compatible with the corresponding point (i.e., the point with the same barycentric coordinates) in its dual. In fact this is true even after a cyclic permutation of the vertices: $\forall x, y, z \in \mathbb{R}$,

$$xe^{(1)}+ye^{(8)}+ze^{(10)} \,|||\, xe^{(2)}+ye^{(9)}+ze^{(7)},\ xe^{(7)}+ye^{(2)}+ze^{(9)},\ xe^{(9)}+ye^{(7)}+ze^{(2)}.$$

This is immediate from the calculation [CSa, Pair_of_Level-1_T3s.nb]:

$$\begin{aligned}
&\det\Big((xe^{(1)}+ye^{(8)}+ze^{(10)})-(xe^{(2)}+ye^{(9)}+ze^{(7)})\Big)\\
&=\det\Big((xe^{(1)}+ye^{(8)}+ze^{(10)})-(xe^{(7)}+ye^{(2)}+ze^{(9)})\Big)\\
&=\det\Big((xe^{(1)}+ye^{(8)}+ze^{(10)})-(xe^{(9)}+ye^{(7)}+ze^{(2)})\Big)\\
&=0.
\end{aligned}$$

Thus, in particular, each node of $\tau_{1,8,10}$ is compatible with every node of $\tau_{2,7,9}$ (and vice versa). Since the nodes of a T_3 are pair-wise compatible it follows that these six nodes (i.e. in the notation of Section 4, $e_{1,8}$, $e_{8,10}$, $e_{10,1}$, $e_{2,9}$, $e_{9,7}$ and $e_{7,2}$) are pair-wise compatible (see Figure 7.2, note that the figure is schematic; in fact τ and $r_0\tau$ share the same barycenter). We conclude that:

$$\mathcal{C}(\{e_{1,8}, e_{8,10}, e_{10,1}, e_{2,9}, e_{9,7}, e_{7,2}\}) \subset \mathcal{R}(\{e_1, e_2, e_7, e_8, e_9, e_{10}\}).$$

Each point in this convex hull is attained by a lamination of the nodes of $\tau_{1,8,10}$ and $\tau_{2,7,9}$. A simple Mathematica verification [CSa, Dimension.nb] shows that this convex hull is four-dimensional. (Thus the maximum depth of lamination required is also four, cf. proof of Theorem 2.11.)

Note that when $\varepsilon \leqslant \delta$, from (7.1),

$$\mathcal{C}(\{e_{1,8}, e_{8,10}, e_{10,1}, e_{2,9}, e_{9,7}, e_{7,2}\}) \subset \partial\mathcal{R}(\mathcal{E}). \tag{7.2}$$

7.2 Level-2 T_3s and related microstructures

Next we construct new T_3s from the nodes of the T_3s in $\mathcal{T}$. We refer to the former T_3s as Level-1 T_3s and to the new T_3s as Level-2 T_3s. Level-2 T_3s allow us to construct a five-dimensional set of T_3s, see Construction 7.5 below.

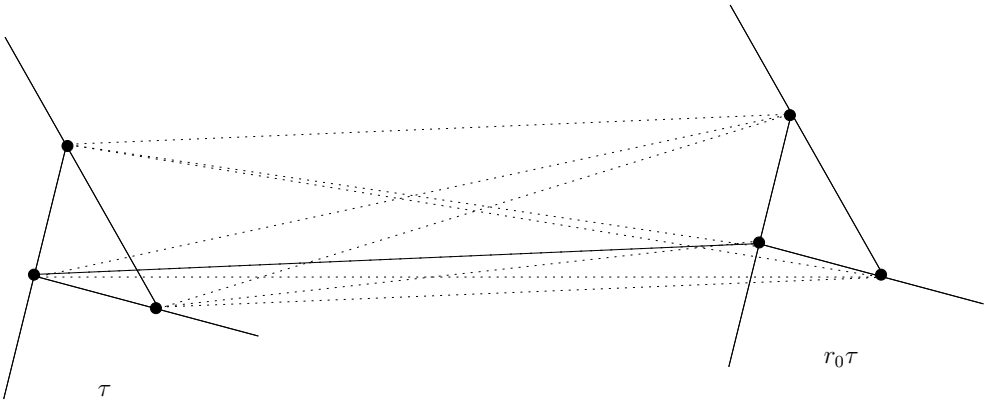


Fig. 7.2: Schematic representation of the four-dimensional set of laminates of nodes of T_3s constructed in Example 7.3.

Construction 7.4 Let $\tau \in \mathcal{T}$ and let $\tau_1, \tau_2, \tau_3 \in \mathcal{T}$ be chosen such that, in Figure 7.1, the line joining τ and τ_i is an edge of the cube for $i = 1, 2, 3$ (thus $\tau_i = r_j^{\pm 1}\tau$ for some $j = 1, 2, 3$). Note that the set $\{\tau_1, \tau_2, \tau_3\}$ is invariant under any element of S_4 that leaves $\{\tau, r_0\tau\}$ invariant (these are rotations of $\frac{2\pi}{3}$ through the major diagonal formed by τ and $r_0\tau$). Let r be an element of this group (i.e., one of two such rotations). Now let n_1 be a node of τ_1. Then n_1, rn_1, r^2n_1 form a symmetric T_3 with distinct nodes. Similarly for n_2, rn_2, r^2n_2 and n_3, rn_3, r^2n_3. This is illustrated in Figure 7.3.

Proof We show that n_1, rn_1, r^2n_1 form a T_3 explicitly for $\tau = \tau_{3,8,11}$, $\tau_1 = \tau_{1,8,10}$, $\tau_2 = \tau_{2,5,11}$ and $\tau_3 = \tau_{3,6,9}$; the result for the other 3-tuples follows by symmetry.

Since $n_1 \in \tau_{1,8,10}$, it has the barycentric representation $xe^{(1)} + ye^{(8)} + ze^{(10)}$ for some $x, y, z \in [0, 1]$ with $x + y + z = 1$. Then, as can be easily checked (Table 5.5),

$$\{rn_1, r^2n_1\} = \{xe^{(5)} + ye^{(11)} + ze^{(2)}, xe^{(9)} + ye^{(3)} + ze^{(6)}\}.$$

(Note the order of the vertices.) It can be verified [CSa, Level-2_T3s.nb] that

$$\begin{aligned}
&\det\Big((xe^{(1)} + ye^{(8)} + ze^{(10)}) - (xe^{(5)} + ye^{(11)} + ze^{(2)})\Big) \\
&= \det\Big((xe^{(5)} + ye^{(11)} + ze^{(2)}) - (xe^{(9)} + ye^{(3)} + ze^{(6)})\Big) \\
&= \det\Big((xe^{(9)} + ye^{(3)} + ze^{(6)}) - (xe^{(1)} + ye^{(8)} + ze^{(10)})\Big) \\
&\neq 0.
\end{aligned}$$

Thus, by Lemma 4.3, Remark 4.7 and (5.3), n_1, rn_1, r^2n_1 form a symmetric T_3. (From Remark 4.7 it would have sufficed to check that one of the determinants

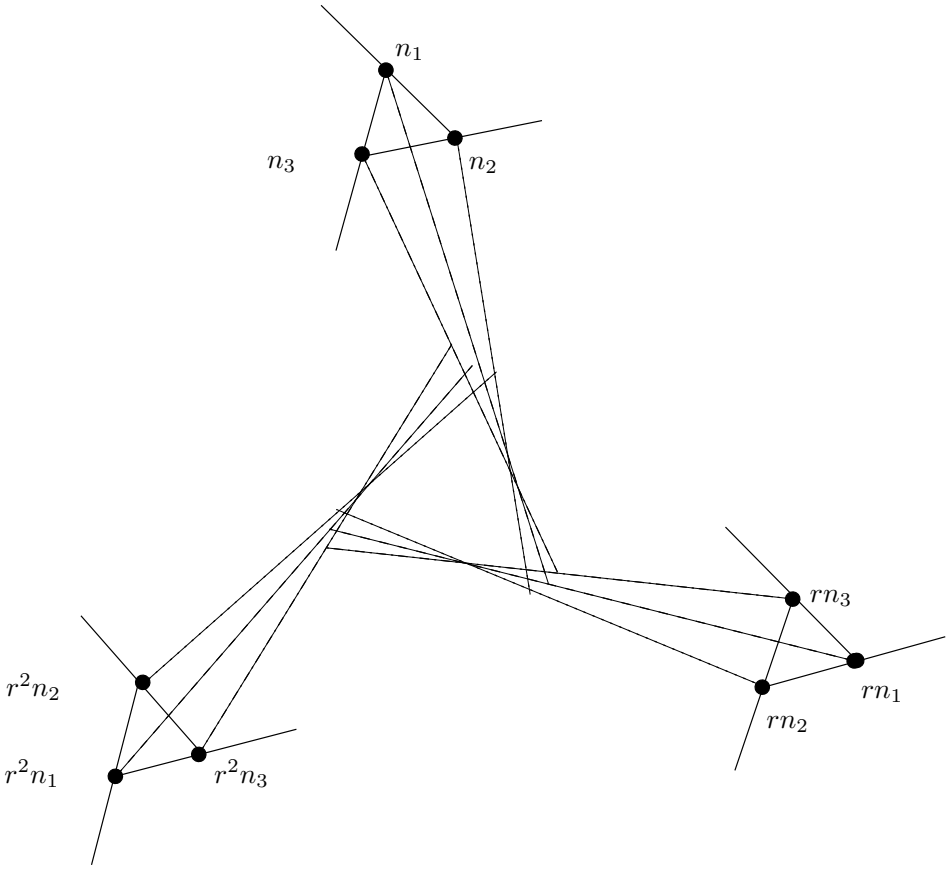


Fig. 7.3: Level-2 T_3s.

above is non-zero.) To show that the nodes of this T_3 are distinct it suffices to check that the barycentre of the T_3 is incompatible with (one of) its nodes (cf. proof of Lemma 7.1). From [CSa, Level-2_T3s.nb]:

$$xe^{(1)} + ye^{(8)} + ze^{(10)},\ xe^{(5)} + ye^{(11)} + ze^{(2)},\ xe^{(9)} + ye^{(3)} + ze^{(6)}$$
$$\not\parallel \frac{1}{3}\left((xe^{(1)} + ye^{(8)} + ze^{(10)}) + (xe^{(5)} + ye^{(11)} + ze^{(2)}) + (xe^{(9)} + ye^{(3)} + ze^{(6)})\right).$$

Which completes the proof.

Since there are eight choices of τ and three choices of n_1 for each choice of τ, by this construction we obtain 24 T_3s.

Finally Example 7.3 and Construction 7.4 can be combined to construct a five-dimensional set of T_3s whose vertices are themselves laminates of nodes of (level-1) T_3s.

Construction 7.5 Let $\tau \in \mathcal{T}$ and let $\tau_1, \tau_2, \tau_3 \in \mathcal{T}$ and $r \in S_4$ be as in Construction 7.4 above. Let $n_{1,i}$ and $n'_{1,i}$, $i = 1, 2, 3$ be the nodes of τ_1 and its dual respectively. Pick $\mu_i, \mu'_i \in [0, 1]$ such that $\sum_{i=1}^{3} \mu_i + \sum_{i=1}^{3} \mu'_i = 1$ and let

$$p_1 = \sum_{i=1}^{3} \mu_i n_{1,i} + \sum_{i=1}^{3} \mu'_i n'_{1,i}.$$

Note that p_1 is an element of the four-dimensional set constructed in Example 7.3 and thus can be attained by a lamination of $n_{1,i}, n'_{1,i}$, $i = 1, 2, 3$. We assert that p_1, rp_1, r^2p_1 form a symmetric T_3. The union of the T_3s as p_1 varies yields a five-dimensional set. When $\varepsilon \leqslant \delta$ from (7.2), this set intersects the boundary of the symmetrised rank-one convex hull of $\mathcal{E}$.

Proof A Mathematica calculation [CSa, Level-2_T3s.nb] shows this explicitly for $\tau_1 = \tau_{1,8,10}$, $\tau_2 = \tau_{2,5,11}$ and $\tau_3 = \tau_{3,6,9}$ (i.e., $\tau = \tau_{3,8,11}$), the construction for the other 3-tuples is similar.

To see that the set of T_3s constructed here is five-dimensional, it suffices to note that p_1 is picked from a four-dimensional set which, not being closed under r, does not contain the T_3s formed by p_1, rp_1, r^2p_1. It follows that the union of the T_3s (as p_1 varies) constructed here is a five-dimensional set.

It is natural at this point to ask whether the nodes of level-2 T_3s form level-3 T_3 and, more generally, whether the nodes of level-n T_3s from level-$(n + 1)$ T_3s. We postpone these questions to [CSb] and instead conclude by considering some implications of the results presented here.

8 Conclusions

8.1 Mathematical comments

While we have, in the later half of this paper, focused on monoclinic-I martensite, it is clear that our general strategy can, in principle, be applied to any finite set in $\mathcal{S}_c^{3\times3}$; indeed in [CSb] we apply it also to monoclinic-II martensite. Here we briefly comment on the two main components of our strategy, namely an understanding of the algebraic structure of symmetrised rank-one convex cones, and an understanding of the polytope structure of the given set.

The algebraic structure of symmetrised rank-one convex cones. While we have a complete understanding of symmetrised rank-one convexity in two-dimensions (Sections 3 and 4, and [CSc]), the algebraic structure of symmetrised rank-one convex cones is not yet sufficiently well understood in higher dimensions. A key missing ingredient is a characterisation, in terms of canonical forms, of real cubic polynomials in several variables. This problem in invariant theory seems unsolved for three and more variables. The fruitfulness of our approach in two-dimensions suggests that it might be valuable to more fully explore the algebraic aspects of symmetrised rank-one convexity.

When $\varepsilon < \delta$ we demonstrate the existence of T_3s that attain points on the boundary of $\mathcal{C}(\mathcal{E})$, more precisely, that attain points on the four-dimensional facets of $\mathcal{C}(\mathcal{E})$. Though (as a Mathematica calculation [CSa, Facet-T3Pair.nb] shows the T_3s do not belong to the three-dimensional facets (of the four-dimensional facets) of $\mathcal{C}(\mathcal{E})$, we suspect that the symmetrised rank-one convex hull of monoclinic-I martensite is strictly larger than the lamination hull. If so, the question arises as to how much larger it is. In terms of dimensions a perturbation argument shows that $\mathcal{R}(\mathcal{E})\setminus\mathcal{L}(\mathcal{E})$ would be at least two-dimensional. In fact we suspect that it is full (i.e., five) dimensional.

Convex polytopes. Since the convex hull of any finite set is a convex polytope, it is natural that an attempt to determine the semi-convex hull of a finite sets takes advantage of the structure of the convex polytopes they generate. This seems not to have been considered in the literature except for Theorem 2.11. Lemma 6.3 and Remark 6.4 demonstrate the counter-intuitive behaviour of high-dimensional polytopes and thus the usefulness of knowledge of the theory of convex polytopes.

Moreover, when, as in the example of monoclinc-I martensite considered here, the faceting structure of the polytope depends on the material parameters, it might be expected that qualitative features of the semi-convex hulls and envelopes depend on the material parameters as well. If so, this heightens the possible utility of these polytopes for evaluating semi-convex hulls and envelopes.

8.2 Implications for mechanics

Two kinds of monoclinic-I martensite. Curiously, all cubic-to-monoclinic-I materials that we are aware of are monoclinic-Ia martensites (i.e., those for which $\varepsilon < \delta$), see Table 5.2. It is natural to ask whether monoclinic-I martensite recovers more strains (modulo appropriate normalisation of the lattice parameters) as $\varepsilon - \delta$ approaches zero (with $\varepsilon = \delta$ being the ideal), and whether monoclinic-Ib martensites (i.e., those for which $\varepsilon > \delta$) would demonstrate greater shape memory effect.

Monoclinic-II martensite. We have reason to believe that there are multiple kinds of monoclinic-II martensite as well. We hope to settle this question in [CSb].

As can be easily verified (eg. [Bha03]), the compatibility relations between the twelve transformation strains of monoclinic-II martensite are identical to those between the twelve transformation strains of monoclinic-I martensite. Then, with the help of Lemma 4.3, exactly as for monoclinic-I martensite, eight T_3s can be formed from these strains. This positively answers the question raised in [BFJK94, p863] as to whether T_3s can be formed from the twelve transformation strains of monoclinic-II martensite. Indeed Lemma 4.3 presents an elementary test by which this question can be answered for any three-tuple of strains that have the same trace.

Material	λ	$(\alpha-\beta)\delta+\varepsilon^2-\delta^2$
NiTi	0.6830	0.0024
TiNiCu	0.6683	0.0021
CuZr	0.0396	−0.0015

Table 8.1: λ and $(\alpha-\beta)\delta+\varepsilon^2-\delta^2$ for the T_3s in $\mathcal{T}$ for NiTi, CuZr and TiNiCu.

Special parameters. Throughout this paper, including in the (non-numerical) Mathematica computations, we have assumed the lattice parameters to be generic except that we considered the case $\varepsilon = \delta$. We did identify one special case, $(\alpha-\beta)\delta+\varepsilon^2-\delta^2 = 0$, in which all twelve strains of monoclinic-I martensite are pair-wise compatible.

The question arises as to whether a material recovers more strains as $(\alpha-\beta)\delta+\varepsilon^2-\delta^2$ approaches zero. We suggest another parameter of importance, $\lambda := \lambda_{12} = \lambda_{23} = \lambda_{31}$ (Definition 4.6) which however appears related to $(\alpha-\beta)\delta+\varepsilon^2-\delta^2$ for the three materials considered in Table 8.1.

Our reasoning is that as λ becomes close to either 0 or 1, the nodes of a T_3 become closer to its vertices and the energetic penalty for a T_3 microstructure being approximated by a finite-rank laminate becomes smaller. Indeed, instead of constructing a finite-rank laminate from the three nodes of a T_3, it suffices to move only *one* of the vertices to a node.

As Table 8.1 shows $\lambda = 0.0396$ for CuZr. We hypothesise that for this material the symmetrised lamination convex hull is very close to the convex hull and thus the convex hull is a very good approximation to all its semi-convex hulls. The same would apply to the (semi-)convex envelopes of the corresponding energy density as well. A similar reasoning might explain the remarkable closeness between the symmetrised lamination convex hull and the convex hull for CuAlNi (a monoclinic-II martensite) observed in [GHH07].

Microstructure corresponding to T_3s. For monoclinic-I martensite with $\varepsilon < \delta$ we have shown that there exists a five-dimensional set of T_3s which reaches the boundary of $\mathcal{C}(\mathcal{E})$. This raises the question as to whether the microstructures experimentally observed for strains in this set are laminate approximations to T_3 microstructures. We wonder too if experimental observations of such microstructures would provide insight into mechanisms governing microstructure formation (dynamics) and the role of surface energy.

Acknowlegements. This research was supported by the Royal Society (International Joint Project "Symmetrised rank-one convex hull of monoclinic martensite"). It was initiated while the authors were at the Max Planck Institute for Mathematics in the Sciences, Leipzig and continued while AS was at the Department of Mathematics, University of Erlangen-Nuremberg, the Hausdorff Center for Mathematics and the Institute for Applied Mathematics, University of Bonn. IVC thanks these institutes and the Institute for Mathematics, University of Würzburg for hospitality during visits. IVC was introduced to the problem of determining the semi-convex hulls of monoclinic-I martensite

when Sanjay Govindjee and Valery Smyshlyaev visited Kaushik Bhattacharya at Caltech. We thank Kaushik Bhattacharya, Richard James, Robert Kohn and Stefan Müller for helpful discussions. We thank the referees for helpful comments, for suggesting the name "wave convex", and for bringing [Tar79, Mur07] to our attention.

References

Bar03. Alexander Barvinok, *A course in convexity*, Graduate studies in mathematics, American Mathematical Society, 2003. (Cited on page(s) 6, 27.)

BFJK94. Kaushik Bhattacharya, Nikan B Firoozye, Richard D James, and Robert V Kohn, *Restrictions on microstructure*, Proceedings of the Royal Society of Edinburgh. Section A. Mathematics **124** (1994), no. 5, 843–878. (Cited on page(s) 3, 11, 12, 34.)

Bha93. Kaushik Bhattacharya, *Comparison of the geometrically nonlinear and linear theories of martensitic transformation*, Continuum Mechanics and Thermodynamics **5** (1993), no. 3, 205–242. (Cited on page(s) 7.)

Bha03. ———, *Microstructure of martensite: Why it forms and how it gives rise to the shape-memory effect*, Oxford series on materials modelling, Oxford University Press, 2003. (Cited on page(s) 16, 26, 34.)

BJ87. John M Ball and Richard D James, *Fine phase mixtures as minimizers of energy*, Archive for Rational Mechanics and Analysis **100** (1987), no. 1, 13–12. (Cited on page(s) 2.)

BK97. Kaushik Bhattacharya and Robert V Kohn, *Elastic energy minimization and the recoverable strains of polycrystalline shape-memory materials*, Archive for Rational Mechanics and Analysis **139** (1997), no. 2, 99–180. (Cited on page(s) 2, 16.)

Brø82. Arne Brøndsted, *An introduction to convex polytopes*, Graduate texts in mathematics, Springer, 1982. (Cited on page(s) 6, 24.)

CSa. Isaac Vikram Chenchiah and Anja Schlömerkemper, *Electronic supplementary material to this article available at http://www.maths.bris.ac.uk/ maivc/*. (Cited on page(s) 4, 15, 16, 17, 19, 20, 21, 22, 23, 24, 25, 26, 27, 30, 31, 32, 33, 34.)

CSb. ———, *Monoclinic martensite: Recoverable strains, zero-energy microstructures and relaxed energy*. (Cited on page(s) 3, 4, 18, 33, 34.)

CSc. ———, *Symmetrised rank-one convexity in two-dimensional affine subspaces of three-dimensional strains*. (Cited on page(s) 3, 4, 11, 33.)

Dac07. Bernard Dacorogna, *Direct methods in the calculus of variations*, 2 ed., Applied mathematical sciences, Springer, 2007. (Cited on page(s) 3, 6.)

Ewa96. Günter Ewald, *Combinatorial convexity and algebraic geometry*, Springer, 1996. (Cited on page(s) 6, 24.)

GHH07. Sanjay Govindjee, Klaus Hackl, and R Heinen, *An upper bound to the free energy of mixing by twin-compatible lamination for n-variant martensitic phase transformations*, Continuum Mechanics and Thermodynamics **18** (2007), no. 7-8, 443–453. (Cited on page(s) 35.)

Grü03. Branko Grünbaum, *Convex polytopes*, 2 ed., Graduate texts in Mathematics, Springer, 2003. (Cited on page(s) 6.)

Gru07. Peter M Gruber, *Convex and discrete geometry*, Grundlehren der mathematischen Wissenschaften, vol. 336, Springer, 2007. (Cited on page(s) 6.)

Gur64. Grigorii Borisovich Gurevich, *Foundations of the theory of algebraic invariants*, P. Noordhoff, 1964. (Cited on page(s) 10.)

HGSN07. G Hall, Sanjay Govindjee, P Sittner, and V Novak, *Simulation of cubic to monoclinic-II transformations in a single crystal Cu–Al–Ni tube*, International Journal of Plasticity **23** (2007), no. 1, 161–182. (Cited on page(s) .)

HS99. Kevin F Hane and Thomas W Shield, *Microstructure in the cubic to monoclinic transition in titanium-nickel shape memory alloys*, Acta Materialia **47** (1999), no. 9, 2603–2617. (Cited on page(s) 16, 19.)

Koh91. Robert V Kohn, *The relaxation of a double-well energy*, Continuum Mechanics and Thermodynamics **3** (1991), no. 3, 193–236. (Cited on page(s) 5.)

Kre03. Carl-Friedrich Kreiner, *Algebraic methods for convexity notions in the calculus of variations*, Master's thesis, Technische Universitaet Muenchen, 2003. (Cited on page(s) 2, 7, 11, 14.)

KS81. K M Knowles and D A Smith, *The crystallography of the martensitic-transformation in equiatomic nickel-titanium*, Acta Metallurgica et Materialia **29** (1981), no. 1, 101–110. (Cited on page(s) 16.)

KZC04. Carl-Friedrich Kreiner, Johannes Zimmer, and Isaac Vikram Chenchiah, *Towards the efficient computation of effective properties of microstructured materials*, Comptes Rendus Mecanique **332** (2004), no. 3, 169–174. (Cited on page(s) 2.)

Mül99. Stefan Müller, *Variational models for microstructure and phase transitions*, Calculus of variations and geometric evolution problems: Lectures given at the 2nd session of the Centro Internazionale Matematico Estivo (CIME) held in Cetraro, Italy, June 15–22, 1996 (Fabrice Bethuel, Gerhard Huisken, Stefan Muller, and Klaus Steffen, eds.), Springer, 1999, pp. 85–210. (Cited on page(s) 6.)

Mur07. François Murat, *Compacité par compensation: Condition nécessaire et suffisante de continuité faible sous une hypothèse de rang constant*, Annali della Scuola Normale Superiore di Pisa - Classe di Scienze, Sér. 4 **8** (2007), no. 1, 69–102. (Cited on page(s) 6, 36.)

NSNS90. Tae Hyun Nam, Toshio Saburi, Yoshiyuki Nakata, and Ken'ichi Shimizu, *Shape memory characteristics and lattice deformation in Ti-Ni-Cu alloys*, Materials Transactions Jim **31** (1990), no. 12, 1050–1056. (Cited on page(s) 16.)

Olv99. Peter J Olver, *Classical invariant theory*, Cambridge University Press, 1999. (Cited on page(s) 10.)

OSS71. K Otsuka, T Sawamura, and K Shimizu, *Crystal structure and internal defects of equiatomic TiNi martensite*, Physica Status Solidi (A) **5** (1971), no. 2, 457–470. (Cited on page(s) 16.)

PZ98. M Pitteri and G Zanzotto, *Generic and non-generic cubic-to-monoclinic transitions and their twins*, Acta Materialia **46** (1998), no. 1, 225–237. (Cited on page(s) 15.)

Roc96. Ralph Tyrell Rockafellar, *Convex analysis*, Princeton landmarks in mathematics, Princeton University Press, 1996. (Cited on page(s) 6.)

SB97. Y Shu and Kaushik Bhattacharya, *The influence of texture on the shape-memory effect in polycrystals*, Acta Materialia **46** (1997), no. 15, 5457–5473. (Cited on page(s) 16.)

SJ05. László Székelyhidi Jr., *Rank-one convex hulls in* $\mathbb{R}^{2\times 2}$, Calculus of Variations and Partial Differential Equations **22** (2005), no. 3, 253–281. (Cited on page(s) 11.)

SS98a. J W Seo and D Schryvers, *TEM investigation of the microstructure and defects of CuZr martensite. Part I: Morphology and twin systems*, Acta Materialia **46** (1998), no. 4, 1165–1175. (Cited on page(s) 16.)

SS98b. ———, *TEM investigation of the microstructure and defects of CuZr martensite. Part II: Planar defects*, Acta Materialia **46** (1998), no. 4, 1177–1183. (Cited on page(s) 16.)

Sve92. Vladimír Sverák, *Rank-one convexity does not imply quasiconvexity*, Proceedings of the Royal Society of Edinburgh, A: Mathematics **120** (1992), no. 1-2, 185–189. (Cited on page(s) 3.)

Tar79. Luc Tartar, *Compensated compactness and applications to partial differential equations*, Nonlinear Analysis and Mechanics: Heriot-Watt Symposium, Volume IV (R Knops, ed.), Pitman, 1979. (Cited on page(s) 6, 36.)

Tar93. ———, *Some remarks on separately convex functions*, Microstructure and phase transition (David Kinderlehrer, Richard D James, Mitchell Luskin, and Jerry L Ericksen, eds.), Springer, 1993, pp. 191–204. (Cited on page(s) 11.)

TZ08. Qi Tang and Kewei Zhang, *Bounds for effective strains of geometrically linear elastic multiwell model*, Journal of Mathematical Analysis and Applications **339** (2008), no. 2, 1264–1276. (Cited on page(s) 2, 8.)

Wei88. David A Weinberg, *The affine classification of cubic curves*, Rocky Mountain Journal of Mathematics **18** (1988), no. 3, 655–664. (Cited on page(s) 10.)

Zha06. Kewei Zhang, *Estimates of quasiconvex polytopes in the calculus of variations*, Journal of Convex Analysis **13** (2006), no. 1, 37–50. (Cited on page(s) 2, 8.)
Zie94. Günter M Ziegler, *Lectures on polytopes*, Springer, 1994. (Cited on page(s) 6, 24.)